ECOMORPHOLOGY AND ONTOGENY MODULATE THE MECHANICAL PROPERTIES OF SHARK SKIN

Madeleine E. Hagood[1*], Joseph R.S. Alexander[1], Michelle Passerotti[2], and Marianne E. Porter[1]

[1]*Department of Biological Sciences, Florida Atlantic University, Boca Raton, FL, USA*
[2]*National Oceanic and Atmospheric Administration Fisheries Apex Predators Program*

Abstract

Shark skin is a biological composite of dermal denticles embedded in a multilayered network of collagen fibers. Variation of skin morphology (dermal denticles and collagen fibers) is observable among species, body regions, and developmental stages, and has been shown to relate to skin mechanics. The orientation of collagen fibers results in mechanical anisotropy; shark skin is more extensible when stressed longitudinally (anteroposterior) and stiffer when stressed perpendicularly (dorsoventral). To evaluate the impact of ecological and ontogenetic factors on mechanical behavior, we tested shark skin in uniaxial tension to failure and calculated the tensile strain and mechanical properties (strength, stiffness, and toughness) from 20 species, and quantified the effects of ecomorphotype and ontogeny, as well as stress axis and body region. The bonnethead shark *Sphyrna tiburo* was used as a case study to quantify mechanics in a single species across an ontogenetic series. We analyzed the skin morphology and correlated this with mechanical behavior to understand the mechanisms that regulate skin function. Across ecomorphotypes, shark skin from deeper-water, non-migratory species (Ecomorphotype E) was stronger and tougher than skin from small-bodied, non-migratory species (Ecomorphotype B), and medium-bodied, migratory species (Ecomorphotype C) had stiffer skin than large-bodied, migratory species (Ecomorphotype D). We found skin from mature sharks was stronger, stiffer, tougher, and more extensible than skin from pups. These results indicate that ontogeny and ecomorphotype impact skin mechanics among sharks. Despite morphological diversity, aspects of skin morphology appear to play less of a role in regulating mechanical function.

1. Introduction

Shark skin is a layered composite containing dermal denticles and collagenous fibers that may function as an external tendon, storing and releasing elastic energy to reduce the metabolic cost of swimming [1,2,3,4,5]. The dermis is covered by the crowns of protruding dermal denticles (placoid scales), tooth-like structures of dentine and enameloid [6]. In the dermis there are two layers, the superficial stratum laxum and the deep stratum compactum, the latter of which is thicker, contains more collagen fiber layers, and houses the roots of the dermal denticles [1,5,6,7]. Layers of collagen fibers in the stratum compactum are oriented at overlapping left- and right-hand helices and are intersected by perpendicular-running Sharpey's fibers that anchor the denticles [1,2,5]. The arrangement of collagen fibers in shark skin is conserved among species, ranging from 40–60º in the mid-body, relative to the longitudinal (anteroposterior) body axis [1,2]. In a fiber-reinforced pressurized cylinder model, fiber angles of ~54º are suited for maintaining optimum stress forces along both the longitudinal and hoop (circumferential or dorsoventral) stress axes [1,2,3,8].

Essentially, shark bodies function as pressurized cylinders and the collagen fiber network reduces skin hypertension during rapid swimming [2,3,4,8,9,10]. The skin is connected to the musculoskeletal system and the combined mechanical properties may impact the kinematic behavior by resisting stress or storing elastic energy to release during undulation [2,11,12]. Internal hydrostatic pressure changes are modulated by skin extension and stiffening during bending, so the skin functions to reduce energetic work and improve swimming performance [2,4,9,10]. The collagen fiber orientation in shark skin impacts mechanical properties, such as tensile strain and stiffness, and results in anisotropy, where skin exhibits different behaviors along varying stress axes. Along the axis of undulation (longitudinal), shark skin is more extensible, allowing for improved axial bending. Conversely, skin is stiffer when stressed along the hoop axis to maintain internal hydrostatic pressure while permitting flexibility [3,4,5,8,13].

The mechanical anisotropy of shark skin has been shown to be a direct result of the arrangement of the collagen fiber network [1,2]. Due to this anisotropy, shark skin modulates bending and flexing of the

body during swimming and has been hypothesized to function as an exotendon [2]. A tendon (here, the skin) facilitates efficient force transmission along the body and reduces locomotor work through its attachments with the vertebrae and muscles, which act in sequence to produce movement [2,3]. This has been demonstrated *in vivo* in a single shark; stimulated skin stiffened in response to pressure changes, synonymous with faster swimming [2]. The exotendon hypothesis was developed with data from two carcharhinid sharks (one living lemon shark *Negaprion brevirostris* and one dead dusky shark *Carcharhinus obscurus*). Anisotropic mechanical data from adult spadenose shark *Scoliodon laticaudus* skin has since provided support for the hypothesis [5]. More recently, data from three juvenile carcharhinid shark species' skin (silky shark *Carcharhinus falciformis*; bull shark *C. leucas*; and bonnethead shark *Sphyrna tiburo*) provided further support of mechanical anisotropy and indicated that mechanical behaviors vary among these species which have various ecologies and niches, swim at different speeds, and have unique body sizes at maturity [13]. In total, there are mechanical data from shark skin (tested along both axes of stress) from just four species, so research into changes among mechanical behaviors across ecologically distinct groups or ontogenetic stages is largely unexplored.

Morphological aspects of shark skin have been shown to impact mechanical properties among species, regions of the body, and between sexes [1,2,5,13,14,15,16,17]. Along an individual shark's body, skin thickness and fiber organization vary [1,2,5]. For example, collagen fibers (relative to the longitudinal axis) in spadenose shark skin form a wider range of angles (50–70˚) in the anterior body region and have greater fiber waviness, resulting in greater extension during tensile testing [5]. Skin from the rounder, posterior body of the spadenose shark contains a narrower fiber angle range (50–55˚), smaller fiber angles, and more compact fibers, which behave mechanically stiffer and stronger to facilitate large volume changes from muscle contractions that may reduce swimming efficiency as the body narrows towards the tail [5]. Skin thickness also varies among body regions, with a greater proportion of collagen fibers and less fiber waviness (indicating less fiber extension) towards the posterior body [5]. Thickness of the stratum compactum layer of the dermis is known to vary among species [1], and mature female blue sharks and lesser-spotted catsharks have thicker skin relative to their male counterparts, a trait thought to provide

protection during mating [14,18]. Among juveniles, female sharks have thicker skin with larger collagen fiber angles compared to males which have thinner, mechanically tougher skin [13].

Dermal denticle density and morphology are diverse and vary among species, body regions, and ontogenetic stages [15,17,18,19,20,21,22,23,24,25,26,27]Functionally, flatter denticles with rounded ridges serve as protective armor for slower-swimming shark species, whereas faster-swimming species have taller denticles with pointed ridges that improve hydrodynamics and reduce drag by creating backflow in the boundary layer [15,19,20,28,29]. Due to the ecologically specific body morphology and behaviors of different shark species, previous studies have utilized the idea of ecomorphotypes to compare species rather than taxonomic or phylogenetic groups. Ecomorphotypes categorize species into functional groups with shared ecological and morphological traits, e.g., migration, swimming speed, size at sexual maturation, and habitat preference (**Table 1**) [30,31]. Here species were categorized as: benthic and non-migratory (Ecomorphotype A), small-bodied and non-migratory (Ecomorphotype B), medium-bodied and migratory (Ecomorphotype C), large-bodied and migratory (Ecomorphotype D), and comparatively deeper-water, medium-bodied, non-migratory sharks (Ecomorphotype E).

In addition to the diversity among species and regional morphologies, dermal denticles vary throughout development. For example, the dermal denticles of Portuguese dogfish *Centroscymnus coelolepis* skin vary morphologically through ontogenetic stages, and denticle volume and surface area are negatively allometric with body length - becoming proportionally less dense with body growth [27]. Ontogenetic changes in dermal denticle morphology have also been reported for roughskin dogfish *C. owstonii* [25] and Pacific spiny dogfish *Squalus suckleyi* sharks [26]. Ontogenetic changes in dermal denticles could alter mechanical behaviors of the skin throughout development. A dense array of overlapping denticles could result in interlocking and may impact the rigidity of the skin, affecting stiffness or toughness [32]. Previous studies have investigated the role of dermal denticles to enhance hydrodynamic efficiency at the boundary layer [15,29], but denticles have been less considered for their relationship with the mechanical properties of shark skin. Among several coastal shark species, the denticle density positively relates to skin stiffness and negatively relates to toughness, indicating that high denticle density may contribute to stiffer skin; although

results were limited to data from skin stressed longitudinally only [33] When denticle density is correlated with mechanical data from shark skin stressed along both axes, the density positively relates to both skin strength and toughness [13]. The role of dermal denticle density in the mechanical properties of the skin among species and throughout ontogeny thus remains unclear.

Currently, little is known about the variation of mechanical behavior among species that experience different ecological constraints on their behavior, habitat specificity or body size – all of which could affect skin mechanics. Variation of skin mechanical behaviors from three shark species suggests there may be further differences among morphologically or ecologically distinct groups [13]. Additionally, previous studies report skin mechanical data from sharks at different ontogenetic stages (mature vs juvenile) [5,13], so results cannot truly be comparable without investigating the variation of mechanical behavior across developmental groups. Therefore, the goals of this study were to: 1) compare shark skin mechanical behavior and morphology among groups of species with similar niches and life strategies (ecomorphotypes) to evaluate functional differences in an ecological framework, 2) quantify the impact of ontogeny on mechanical properties within a single species and across functional groups, and 3) identify potential underlying mechanisms that modulate shark skin function. Based on the literature, we hypothesized that mechanical behaviors would differ relative to species' ecology and morphology, as well as across ontogenetic stages [1,2,5,15,20,27,30]. Among functional ecomorphotypes, we predicted that faster-swimming, migratory, pelagic shark species with streamlined bodies would have stiffer and stronger skin (Ecomorphotypes C and D), whereas slower-swimming, non-migratory, benthic species (Ecomorphotype A) would have tougher skin. We quantified differences in the skin morphology (thickness, collagen fiber angle, and denticle density) and mechanical behaviors (tensile strain, strength, stiffness, toughness) among five ecomorphotypes (represented by 20 species from six families, and three orders) and ontogenetic stages (pup, juvenile, mature) (**Table 1**). We examined the effect of ontogeny across all sharks, and in a single species using bonnethead sharks, and compared the trends of mechanical behavior. We predicted that mechanical properties would increase ontogenetically from pups to mature sharks. We analyzed the correlative relationships between morphology and mechanics to indicate underlying mechanisms that

moderate shark skin function.

2. Methods

2.1. Study specimens

All specimens were collected by the National Oceanographic and Atmospheric Administration (NOAA) Fisheries, Mote Marine Laboratory (Sarasota, FL), Florida Keys Aquarium Encounters, or Florida Fish and Wildlife Conservation Commission, from the Atlantic coast of the United States and the Gulf and Atlantic coasts of Florida, USA. This work was approved by a Florida Atlantic University Tissue Use Protocol (A (T) 17-05). For this study, sample sizes were uneven due to the opportunistic nature of acquiring fresh tissues and the protected or endangered status of some species.

We obtained skin samples from 49 sharks across 20 species, representing six families in three orders [Carcharhiniformes: Carcharhinidae (N=31 sharks, 15 species) and Sphyrnidae (N=12 sharks, 3 species); Lamniformes: Lamnidae (N=2 sharks, 2 species), Alopiidae (N=1 shark, 1 species) and Odontaspididae (N=1 shark, 1 species); Orectolobiformes: Ginglymostomatidae (N=2 sharks, 1 species); **Table 1**]. Based on previous literature, we grouped species into functional categories of ecological and morphological relatedness (ecomorphotypes) [30,31]. Species were grouped by body size (TL) at maturity recorded in the literature for each species: A) benthic, non-migratory sharks; B) small-bodied, non-migratory sharks; C) medium-bodied, migratory sharks; D) large-bodied, migratory sharks; and E) deep-water, medium-bodied, non-migratory sharks. Order Carcharhiniformes (ground sharks) is the most speciose order of sharks and is represented predominantly by Ecomorphotypes B and C. Faster swimming carcharhinid sharks and pelagic species of lamnid sharks (Order Lamniformes, mackerel sharks) which have large, round bodies comprise Ecomorphotype D. Order Orectolobiformes (carpet sharks) is a small order that includes benthic species like nurse sharks *Ginglymostoma cirratum* (family Ginglymostomatidae), which have more dorsoventrally compressed bodies than other species and functional groups compared here and represent Ecomorphotype A (**Table 1**). After collapsing the data (detailed below), the number of values analyzed ranged across ecomorphotype groups from A (10 points), B

(67 points), C (18 points), D (114 points), to E (4 points).

We assigned each shark in this study to one of three ontogenetic categories using individual body size (fork length; FL, cm) assessed with species-specific growth ranges [30,34,35,36,37,38,39,40,41,42,43,44,45,46,47]. Final ontogenetic categories included eight pups (Ecomorphotypes B and D), 28 immature sharks (Ecomorphotypes A, B, C, and D), and 16 mature sharks (Ecomorphotypes B, C, D, and E). Nurse shark (Ecomorphotype A) samples were both from immature males. The lamnid sharks (Ecomorphotype D) included two pups (common thresher shark *Alopias vulpinus* and sand tiger shark *Carcharias taurus*), one juvenile (white shark *Carcharodon carcharias*) and one mature individual (porbeagle shark *Lamna nasus*). The remaining six pups, 25 juvenile sharks and 15 mature sharks were carcharhinid species (Ecomorphotypes B, C, D, and E; **Tables 1 and 3**). Although we did not compare ontogenetic trends within ecomorphotype groups, all three age categories are represented in Ecomorphotypes B and D.

Finally, the bonnethead shark *Sphyrna tiburo* accounted for eight individuals, representing two pups, two immature, and four mature sharks. This sample enabled us to examine the variation of morphology and mechanical properties across an ontogenetic series.

2.2 Tissue preparation

We stored all sharks frozen prior to dissection and removed skin between the first and second dorsal fins, along the lateral side of the body. We performed dissections atop plastic trays to reduce damage to the skin and denticles. We conducted many of these experiments during the global Severe Acute Respiratory Syndrome Coronavirus 2 (SARS-CoV-2) which impacted the workflow, resulting in two preparation protocols, where one included an additional freezer storage step [13]. If possible, we thawed sharks, dissected skin, and then refrigerated the skin for less than 24 hours prior to imaging and mechanical testing [13,33]. When immediate testing was not possible, we dissected the skin and stored tissue frozen for no more than 3–4 months. In this case, we left at least 1 cm of connected muscle tissue intact with the dermis to prevent dehydration and freezing damage. When we fully thawed these samples and cut them, the

remainder of the protocol was consistent: samples were stored in petri dishes and refrigerated for less than 24 hours prior to imaging and mechanical testing.

For all species, we carefully removed muscle tissue from the deepest dermal layer using a scalpel, leaving 1 mm of muscle fiber tissue connected to prevent puncture or damage prior to analyses. Using digital calipers, we measured the skin thickness from the surface of the denticle layer to the deepest layer of collagen fibers for each sample, so the thickness values include the denticles, epidermis, and dermis layers. The thickness of each dermal layer within a sample was not measured. We measured the size of each dissected skin sample with a tape measure and cut the skin into 5x5 cm^2 squares; the number of squares varied according to shark body size or size of the dissected sample (if provided by collaborators) [12]. Skin samples from bonnethead shark pups were 5x5 cm, representing only one square per shark. We categorized skin squares from between the two dorsal fins into body regions based on dorsoventral location and shark body size (FL). Countershading along the lateral side of the body assisted in identifying dorsal (D; darkly shaded), medial (M; gray shaded), and ventral (V; lightly/not shaded) regions (**Fig. S1**). Specimens considered pups were often not large enough to have a medial region, so data from these individuals represent the dorsal and ventral regions only. When all three regions were present (D, M, V), each accounted for approximately 1/3 of the skin sample. Due to the opportunistic nature of skin collection, some of the samples used in this study represent only one region of the body, and this was assessed with dissection notes and skin countershading.

We stored skin fully submerged in elasmobranch Ringer's Solution in petri dishes and kept dishes refrigerated (2.8 °C) to maintain skin hydration prior to mechanical testing [13,33,48]. Sharks were collected opportunistically over time, with the maximum time in the freezer being five years. Before potential use, we assessed sharks for freezer burn, and any samples that were desiccated were not used in this study. There is evidence that freezing may result in the formation of ice crystals that can damage animal (human and porcine) tissues and decrease mechanical strength and stiffness [49]. Although studies examining freezing effects on the mechanical properties of fish skins are lacking, Kennedy *et al.* [50] reported no significant mechanical differences in the skin between frozen and fresh same-species fish, indicating that freezing may not dramatically impact the mechanical properties of fish skins. Among storage methods, it has been noted

212 that freezing poses the least degree of structural and mechanical change to tissues [51]. Previous research
213 examining skin mechanical properties have used frozen specimens, so results in this study are comparable
214 with mechanical data in the literature [13,33,50,52,53,54].
215
216 *2.3. Morphological analyses*
217 To quantify the relationships among skin morphology and mechanical behaviors related to
218 ecomorphotypes, we analyzed the dermal denticles and collagen fiber angles. We imaged whole 5x5 cm^2
219 skin squares using a Leica EZ4W stereoscopic microscope (Leica Microsystems) and analyzed images
220 in ImageJ (NIH) with 1 mm scale bars, as described in Hagood *et al.* [13] (**Fig. 1**). Areas of each square
221 were imaged at random, and any areas of the skin where denticles were damaged or missing were not
222 analyzed. We calculated denticle density (# denticles · mm^{-2}) at various magnifications (10–35x; **Fig. 1A**).
223 The range of magnification was necessary to accurately image denticles, which are known to vary in
224 morphology and density among species and body regions [15,16,17,18,21,24]. We counted the number of
225 denticles that had 60% or more of the crown surface in a 1x1 mm box (created with the line tool and set to
226 scale for each image) for three images per square and averaged those three counts [13]. in the box We
227 imaged collagen fibers at lower magnifications (8–12.5x) and measured four fiber angles (∡ = ° from
228 longitudinal axis, the axis of undulation during swimming) [55] with one ray parallel with the body axis
229 (sometimes not visible) and the other ray extending towards the dorsal or ventral body plane (**Fig. 1B**). We
230 alternated the orientation of the angle rays so that two angles were anteroventral and two were
231 posterodorsal, and averaged those four angles for each square [13]. If necessary, directionality of the
232 longitudinal axis was confirmed with the denticle orientation on the exterior skin surface, as denticle crowns
233 extend longitudinally with the ridges aligned parallel to the flow of swimming. For this study, we imaged
234 410 total squares, calculated 1230 denticle densities, and measured 1640 collagen fiber angles. Of the 410
235 total squares, Ecomorphotype A contributed 23 squares, 65 squares from B, 31 squares from C, 277 squares
236 from D, and 14 squares from E. We further averaged the average density and fiber angle of each square detailed
237 above for a mean denticle density and collagen fiber angle value for each body region of each shark [13].

238

239 *2.4. Tensile testing*

240 In preparation for materials testing, we pressed a custom tool steel die (Henderson Machine
241 Inc., Boca Raton, FL) onto each skin square using a mechanical press (6 ton; Black Bull) to define the four
242 dog-bone-shaped test pieces to be extracted, two oriented along each stress axis: longitudinal
243 (anteroposterior, parallel to the body axis) and hoop (dorsoventral, perpendicular to the body axis) [13].
244 The dog-bone shape has been used previously in tensile testing experiments to concentrate stress at a
245 consistent region of least surface area [5,13,33]. The die was applied to the deep fibrous layer of each skin
246 square, while the superficial denticle layer rested on paper towels and hard plexiglass. When pressed, a die
247 applies pressure along the edges of the indenting shape while leaving the remainder of the sample
248 unchanged. Following the mechanical press, we removed the four dog-bone pieces from the perimeter tissue
249 of the square with a scalpel and trimmed any extraneous fiber and muscle tissue from each piece for tensile
250 testing. Each dog-bone piece was 10 mm long, 5 mm wide at the center, and the thickness (total of denticles
251 and dermal layers) varied per piece. Although the piece dimensions in this study do not coincide with those
252 provided by the ASTM, shark skin is a non-homogenous biological material composed of several distinct
253 layers that does not uniformly distribute stress as a homogenous sample would. Additionally, previous
254 experiments that stressed shark skin in tension using the dog-bone or dumbbell shape did not fit the samples
255 to ASTM dimensions [5,13,33].

256 We measured the width (mm) and thickness (mm) of each dog-bone piece at the center region using
257 digital calipers to ensure accurate standardizations, and lightly blotted pieces with paper towels (to absorb
258 excess Ringer's solution and reduce slipping) prior to each tensile test [13,33,50]. Using tweezers, we
259 inserted individual dog-bone pieces into stainless steel tension clamps of an Instron E1000 Materials
260 Testing System and performed quasi-static uniaxial tensile testing at 2 $mm \cdot s^{-1}$ strain rate [13,33]. Based
261 on preliminary data collection, we performed tensile testing using either a 250 N load cell (non-
262 mature carcharhinid sharks) or 2 kN load cell (all other sharks), with a pre-load requirement of 1 N to
263 ensure each piece was taut at the beginning of the test. During tensile testing, load-displacement curves

were generated and standardized into stress-strain curves by Bluehill Software (Instron, Norwood, MA, USA). Bluehill Software uses the specific dimensions of each dog-bone piece (length, 10 mm; width, ~5 mm, measured prior to each test; thickness, variable, measured prior to each test) to calculate the mechanical properties of each test. For this reason, each mechanical test is independent and does not depend on the measurements from other mechanical tests or the dimensions of the skin sample originally dissected from each shark. When the dog-bone piece did not reach tensile failure, the test was considered unsuccessful and was excluded from the data. The results presented in this manuscript represent 1640 successful tensile mechanical tests.

2.5. Mechanical properties

From all stress-strain curves, we calculated the tensile strain at maximum load (%) and the following mechanical properties: ultimate strength (MPa), Young's Modulus (MPa), and toughness (MPa). Tensile strain (TS; %) is not a mechanical property but is a calculation of the percentage of material displacement, the change in length over the original length ($\epsilon=\Delta L\backslash L$). Tensile strain at maximum load is the percent of extension at the point of maximum load (unstandardized) or greatest stress (standardized) along a curve. Mechanical properties are used as defined in Hagood *et al.* [13]. Ultimate tensile strength (UTS; MPa) is the highest point of a stress-strain curve and represents the greatest tensile stress a material can withstand prior to permanent deformation. Young's Modulus of elasticity (YM; MPa) is measured as the slope (stress/strain) of the linearly increasing region of a curve following the toe region and represents a material's capacity to resist deformation (stiffness). Toughness (MPa) is a measure of the resistance of a material to completely fracture with stress and is calculated as the total area under a stress-strain curve to failure. All calculations used engineering stress (not true stress) since shark skin does not create a linear region after the yield point indicative of strain hardening, although sample deformation at high strains may alter the cross-sectional area and impact measurements.

2.6. Statistical analyses

For statistical analyses, mechanical data for each shark were averaged for both axes of stress (longitudinal, L; hoop, H) in each region of the body (dorsal, D; medial, M; ventral, V) available for testing [13]. After averaging, each shark is represented by no more than six values per variable: dorsal longitudinal mean, dorsal hoop mean, medial longitudinal mean, medial hoop mean, ventral longitudinal mean, ventral hoop mean. Depending on the species and body size, some sharks did not have enough girth for a medial region. Those sharks are represented by four values per variable: two means each from the dorsal and ventral regions. After collapsing these data, we used a sample of 213 values from 49 sharks for statistical analyses (n=4–6 points per variable per shark). For 47 sharks in this study, means were calculated for each stress axis and body region as described above. The remaining two sharks, bonnethead pups, are represented by their raw data. These two individuals were very small, and we could only dissect one skin square per pup, so each resulted in four mechanical tests.

2.6a. General analyses

Data collected did not meet the assumptions necessary to perform parametric analyses (i.e. normal distribution; Shapiro Wilks, $p<0.05$). Accordingly, we used non-parametric Wilcoxon (for two-outcome variables) or Kruskal-Wallis (for three or more outcomes) rank sum tests with JMP Pro 16.2.0 (SAS Institute Inc.; Cary, NC, USA). These analyses rank the distributions of data for each group, rather than using the mean or median of the data. We used Kruskal-Wallis tests to assess significant variability of skin morphology (denticle density, collagen fiber angle, skin thickness) and mechanical behaviors (tensile strain at max load, ultimate strength, Young's Modulus, toughness) among ecomorphotypes (A-E, **Table 1**), ontogenetic stages (pup, immature, mature), and body regions (D, M, V). We used two-tailed Wilcoxon tests to detect differences in the mechanical behaviors between stress axes (L, H) among pooled data and within ecomorphotypes. The latter analysis was used to determine whether the anisotropy of shark skin mechanical behavior is consistent across ecomorphotype groups. We performed a principal components analysis in RStudio to correlate the mechanical and morphological variables and elucidate the mechanisms underlying the form-function relationships in shark skin.

316 With each significance statement, we present the respective H- or Z-score of the non-parametric
317 analysis, the degrees of freedom (d.f.), and the p-value. Significant results ($p \leq 0.05$) of Kruskal-Wallis tests
318 were further evaluated using the Dunn method for all pairwise comparisons with joint ranking to determine
319 within-group differences. In the results, we provide the mean ± s.e.m. in parentheses for comparison with
320 the literature, although statistical analyses were performed using the distributions of the data. For non-
321 significant results ($p > 0.05$), only the p-value is provided.

322 Fork length measurements were unique to each shark, so these were used to account for individual
323 variation among animals. Due to differences in body size among species, FL measurements indicated body
324 size per individual and were used to determine species-specific maturity stages: pup, immature, mature.
325 Pup was defined as any individual that was not free swimming and whose FL was within or below the
326 species-specific birth size range published in the literature. From this, we could assess the impacts of body
327 size and ontogenetic stage separately. Using JMP, we performed bivariate linear regressions between fork
328 length and each of the morphological and mechanical variables to determine if any of these metrics scaled
329 with individual body size. We report the F- and p-values for significant regressions ($p \leq 0.05$), and the p-
330 value only for non-significant regressions ($p > 0.05$).

331

332 *2.6b. Case study: Mechanics of bonnethead shark skin across ontogenetic stages*

333 To examine the variation of mechanical behavior across stages of ontogenetic development, we analyzed
334 the mechanics of shark skin in a single species among pups (N=2, FL=20–20.5 cm, TL=24.5–26 cm),
335 immature (N=2, FL=48–51 cm, TL=58.4–64), and mature (N=4, FL=47–63 cm, TL=60.5–80.8) animals.
336 We chose the single species with the largest number of individuals (N=8) and greatest range of sizes among
337 study specimens: bonnethead sharks *Sphyrna tiburo* (Ecomorphotype B). The ranges overlap between
338 immature and mature groups because body size at maturity varies between sexes of bonnethead sharks,
339 from 61 cm TL among males to 81 cm TL among females [56]. We had the largest sample of bonnethead
340 sharks as they are small-bodied and commonly inhabit shallow waters along the Eastern Gulf and Western
341 Atlantic coasts of Florida, making this species easier to obtain relative to other sharks. Mechanical data

342 from bonnethead shark skin did not meet the necessary assumptions to perform parametric statistics
343 (Shapiro-Wilks, $p<0.05$). We used non-parametric Kruskal-Wallis rank sum tests to compare the
344 distributions of mechanical data (n=32 data points, 4–6 means per variable per shark, as described above)
345 among the three ontogenetic stages. We provide the H score, p-value, and degrees of freedom (d.f.) with
346 each statement of significance ($p\leq0.05$).
347
348 *2.6c. Principal components analysis (PCA)*
349 We performed a principal components analysis to quantify relationships among mechanical
350 behaviors and skin morphology across ecomorphotypes. PCA is useful for bringing together significant
351 individual variables that are already known to correlate by reducing the dimensionality so that the specific
352 patterns are preserved but variables can be viewed along a unified scale. From the raw mechanical and
353 morphological data, we calculated an average denticle density and collagen fiber angle for each of the dorsal
354 and ventral body regions, tensile strain averaged for each longitudinal and hoop stress axis, strength for
355 each axis, stiffness for each axis, and toughness for each axis (12 values) for 10 sharks. Thickness is
356 incorporated into the calculations of mechanical properties, and it was not included in the PCA. However,
357 skin thickness differs between male and female sharks, and data from a combination of both sexes were
358 used in the PCA which may impact the results. Based on prior morphological PCA studies of fish
359 morphology, we averaged data from one shark per species, using data from sexually mature individuals
360 only [31,57,58]. We grouped data from the 10 species (three families, two orders) into their associated
361 ecomorphotypes (B, C, D, and E; **Tables 1 and 3**). For the other 10 species examined in this study
362 (including the nurse shark of Ecomorphotype A), we did not have data from a mature individual to represent
363 in the PCA. We created a matrix of these 120 data values and used the *PCA( )* function of the FactoMineR
364 package, with scale.unit=TRUE to scale the variables to the same unit. We analyzed the underlying
365 correlative relationships of the data in a new three-dimensional space by reducing the variables to smaller
366 components to visualize the grouping of species within the ecological niches [59]. We generated a biplot
367 of principal components (PCs) 1 and 2, to show potential mechanisms of shark skin function among

ecomorphotypes (**Fig. 8**). We could have used a series of binary plots to highlight the morphological and mechanical interplay in skin function, but these plots would have required Bonferroni corrections and used different scales.

3. Results

3.1 Morphological models

The denticle density of shark skin varied significantly among ecomorphotypes (Kruskal-Wallis, $H(4)=44$, $p<0.0001$), ontogenetic groups (Kruskal-Wallis, $H(2)=57$, $p<0.0001$), and body regions (Kruskal-Wallis, $H(2)=7$, $p=0.03$). The denticle densities of shark skin from Ecomorphotypes B (29 ± 1 denticles $\cdot$ mm^{-2}; $p<0.0001$), C (28 ± 4 denticles $\cdot$ mm^{-2}; $p<0.0001$), and D (20 ± 1 denticles $\cdot$ mm^{-2}; $p=0.0008$) were four to six times greater than the denticle density among sharks of Ecomorphotype A (5 ± 1 denticles $\cdot$ mm^{-2}; **Fig. 2A**). The denticle density among Ecomorphotype B was 30% greater compared to Ecomorphotype D ($p<0.0001$). Across all sharks, skin from immature sharks (29 ± 1 denticles $\cdot$ mm^{-2}) contained 30% more denticles per mm^2 than skin from pups (21 ± 1 denticles $\cdot$ mm^{-2}; $p=0.002$) and nearly 2x the denticle density of mature shark skin (16 ± 1 denticles $\cdot$ mm^{-2}; $p<0.0001$; **Fig. 2B**). Additionally, skin from pups was 25% more denticle-dense than skin from mature sharks ($p=0.02$). Across sharks, the denticle density of shark skin from the ventral body region (23 ± 1 denticles $\cdot$ mm^{-2}) was 25% greater than the medial region (18 ± 2 denticles $\cdot$ mm^{-2}; $p=0.03$), and neither differed from the density of the dorsal region (**Fig. 2C**).

Collagen fiber angles did not significantly vary among ecomorphotypes (Kruskal-Wallis, $p=0.15$), ontogenetic groups ($p=0.16$), or body regions ($p=0.6$). A bivariate regression of collagen fiber angle by FL was at significance ($p=0.05$) and trended positively. Due to the conserved range of collagen fiber angles across groups, we show measurements as a supplementary figure only (**Fig. S3**).

The thickness of shark skin varied significantly among ecomorphotypes (Kruskal-Wallis, $H(4)=79$, $p<0.0001$), ontogenetic stages (Kruskal-Wallis, $H(2)=22$, $p<0.0001$), and body regions (Kruskal-Wallis, $H(2)=11$, $p=0.003$). The thickness for shark skin between Ecomorphotypes D (2 ± 0.1 mm) and E (2 ± 0.1

393 mm) was twice that of skin from Ecomorphotype B (1 ± 0.03 mm; $p<0.0001$ and $p=0.008$, respectively)
394 (**Fig. 2D**). Across all individuals, mature sharks (2 ± 0.1 mm) had 24% thicker skin than immature sharks
395 (1 ± 0.1 mm; $p=0.0007$) and 64% thicker skin than pups (1 ± 0.1 mm; $p=0.0001$; **Fig. 2E**). Immature sharks
396 and pups did not differ in skin thickness ($p=0.67$). Pooled together, skin samples from the medial body
397 region (2 ± 0.2 mm) were 30% thicker than samples from the dorsal (1 ± 0.1 mm; $p=0.005$) and ventral (1
398 ± 0.1 mm; $p=0.004$) regions (**Fig. 2F**). A bivariate regression of thickness by FL was significant and positive
399 ($F=194$, $p<0.0001$), indicating that skin thickness increased relative to body size.
400
401 *3.2 Mechanical models*
402 The tensile strain at max load (extensibility, %) of shark skin significantly varied among
403 ecomorphotypes (Kruskal-Wallis, $H(4)=32$, $p<0.0001$). Sharks in Ecomorphotype E (80 ± 7%) had skin
404 nearly four times more extensible than Ecomorphotypes B (23 ± 2%; $p=0.001$) and C (25 ± 3; $p=0.008$),
405 and Ecomorphotype D (36 ± 2%) also had 40% more extensible skin than Ecomorphotype B ($p=0.0002$;
406 **Fig. 3A**). Across all sharks, the tensile strain varied significantly among ontogenetic groups (Kruskal-
407 Wallis, $H(2)=30$, $p<0.0001$); skin from mature (34 ± 2%) and immature (35 ± 3%) sharks was almost twice
408 as extensible as skin from pups (18 ± 1%; $p<0.0001$; **Fig. 3B**). Mature and immature sharks had similarly
409 extensible skin ($p=0.58$). Across all sharks, skin extensibility varied significantly between axes of stress
410 (Wilcoxon, $Z=7$, $p<0.0001$, two-tailed). Shark skin was 34% more extensible when stressed longitudinally
411 (38 ± 2%) than stressed along the hoop axis (25 ± 2%; **Fig. 3.3C**). Across all sharks, the skin was similarly
412 extensible among body regions ($p=0.12$). The bivariate regression of tensile strain by FL was significant
413 and positive ($F=6$, $R^2=0.02$, $p=0.016$; **Fig. 3D**).
414 The ultimate strength of shark skin varied significantly among ecomorphotypes (Kruskal-Wallis,
415 $H(4)=21$, $p=0.0003$; **Fig. 4A**). Shark skin from Ecomorphotype E (80 ± 5 MPa) was four times as strong as
416 Ecomorphotypes B (18 ± 2 MPa; $p=0.002$) and D (20 ± 8 MPa; $p=0.005$). Across all sharks, skin strength
417 significantly varied among ontogenetic groups (Kruskal-Wallis, $H(2)=45$, $p<0.0001$). Mature (25 ± 2 MPa)
418 and immature sharks (22 ± 1 MPa) had skin more than twice as strong as pups (10 ± 1 MPa; $p<0.0001$; **Fig.**

419 **4B**). Skin strength varied significantly between stress axes (Wilcoxon, Z=-4, p<0.0001, two-tailed); skin
420 tested along the hoop axis (24 ± 1 MPa) was 30% stronger than skin tested longitudinally (18 ± 1 MPa; **Fig.**
421 **4C**). Ultimate strength did not significantly vary among body regions when data were pooled across sharks
422 (p=0.14). A bivariate regression of ultimate strength by FL was not significant (p=0.7).
423 Shark skin stiffness (Young's Modulus, MPa) varied significantly among ecomorphotypes
424 (Kruskal-Wallis, H(4)=14, p=0.007), wherein sharks in Ecomorphotype C (187 ± 28 MPa) had 42% stiffer skin
425 than Ecomorphotype D (110 ± 8; p=0.023; **Fig. 5A**). Across all sharks, mature (140 ± 11 MPa; p=0.028) and
426 immature (127 ± 10 MPa; p=0.005) shark skin was 32-38% stiffer than skin from pups (86 ± 9 MPa; **Fig.**
427 **5B**) (Kruskal-Wallis, H(2)=10, p=0.006). Across all sharks, skin stiffness significantly differed between
428 the two stress axes (Wilcoxon, Z=-8, p<0.0001, two-tailed), when stressed along the hoop axis (171 ± 9
429 MPa) shark skin was more than twice as stiff as it was stressed longitudinally (78 ± 9 MPa; **Fig. 5C**). Shark
430 skin stiffness did not significantly vary among body regions (p=0.3). A bivariate regression of stiffness by
431 FL was not significant (p=0.79).
432 The toughness of shark skin varied significantly among ecomorphotypes (Kruskal-Wallis,
433 H(4)=24.5, p<0.0001). Sharks in Ecomorphotype E (43 ± 2 MPa) had significantly tougher skin than those
434 in Ecomorphotypes B (3 ± 0.3 MPa; p=0.0007) and D (6 ± 0.7 MPa; p=0.01; **Fig. 6A**). Regarding further
435 results of toughness, median values are provided as they are less impacted by outliers relative to the mean
436 values and so, better reflect the outcomes of the statistical analyses. Across all sharks, skin toughness varied
437 significantly among ontogenetic stages (Kruskal-Wallis, H(2)=68, p<0.0001; **Fig. 6B**). The median skin
438 toughness of mature sharks (4 ± 1 MPa; p=0.03) was 18% greater than immature sharks (3 ± 1 MPa) and
439 66% greater than pups (1 ± 0.2 MPa; p<0.0001), and skin toughness of immature sharks was more than
440 twice that of pups (p<0.0001). Across all sharks, skin from the medial body region (4 ± 0.3 MPa) had a
441 higher distribution of toughness and was 25% tougher than the dorsal (3 ± 1 MPa, p=0.025) and ventral (3
442 ± 1 MPa, p=0.003) regions (Kruskal-Wallis, (H(2)=11, p=0.004; **Fig. 6C**). Toughness did not differ
443 between stress axes (p=0.1). A bivariate regression of toughness by FL was not significant (p=0.7).
444

445 *3.3 Case Study: The effect of ontogeny on skin mechanical behavior using bonnethead sharks*

446 The tensile strain at max load (extensibility) of bonnethead shark skin varied significantly among
447 ontogenetic groups (Kruskal-Wallis, H(2)=16, p=0.0004). The skin extensibility of mature bonnethead
448 sharks (27 ± 3%) was greater than pups (8 ± 2%; p=0.0003). The skin of immature sharks (18 ± 2%) was
449 also more extensible than pups (p=0.05; **Fig. 8A**). Mature and immature sharks did not differ in skin
450 extensibility (p=1). Bonnethead shark skin was 39% more extensible along the longitudinal axis (26 ± 3%)
451 compared to the hoop axis (16 ± 3%; Wilcoxon test, Z=2.5, p=0.01, two-tailed).

452 The ultimate strength of bonnethead shark skin varied significantly among ontogenetic groups
453 (Kruskal-Wallis, H(2)=20, p<0.0001). The ultimate skin strength of mature bonnethead sharks (26 ± 3 MPa)
454 was more than 26x the skin strength of pups (1 ± 0.1 MPa; p<0.0001). The skin strength of immature sharks
455 (14 ± 3 MPa) also exceeded that of the pups (p=0.05; **Fig. 8B**). Mature and immature sharks did not differ
456 in skin strength (p=0.4).

457 The stiffness (Young's Modulus) of bonnethead shark skin varied significantly among ontogenetic
458 groups (Kruskal-Wallis, H(2)=13, p=0.001; **Fig. 8C**). Mature bonnethead sharks (165 ± 29 MPa) had skin
459 more than four times as stiff as pups (37 ± 6 MPa; p=0.0009). Immature bonnethead sharks (117 ± 28 MPa)
460 had skin nearly three times as stiff as pups, although this difference was not significant (p=0.06). Immature
461 and mature bonnethead sharks had similarly stiff skin (p=1). Bonnethead shark skin was more than twice
462 as stiff when stressed along the hoop axis (175 ± 23 MPa) as along the longitudinal axis (69 ± 23 MPa;
463 Wilcoxon test, Z=-3, p=0.01, two-tailed).

464 The skin toughness of bonnethead sharks varied significantly among ontogenetic groups (Kruskal-
465 Wallis, H(2)=20, p<0.0001; **Fig. 8D**). Mature bonnethead sharks (5 ± 1 MPa) had skin 50x tougher than
466 pups (0.1 ± 0.01 MPa; P<0.0001), and similar skin toughness as immature sharks (p=0.3). Skin from
467 immature sharks (2 ± 0.4 MPa) was 20x as tough as pup skin, but this difference was not significant
468 (p=0.06).

469 The denticle density of bonnethead shark skin varied significantly among ontogenetic groups and
470 immature sharks (53 ± 5 denticles · mm^{-2}; p<0.0001) had nearly twice as many denticles per square mm as

mature sharks (27 ± 2 denticles · mm^{-2}) (Kruskal-Wallis, H(2)=18, p=0.0001; **Fig. 8E**). Bonnethead pups (28 ± 0.4 denticles · mm^{-2}) had intermediate denticle density (p=0.1). Collagen fiber angles in the skin of bonnethead sharks did not significantly vary among ontogenetic groups (p=0.07).

3.4 Principal Components Analysis

Based on our criteria evaluating only one mature shark per species, data from a subset of 10 individuals (nine carcharhinid species and one lamnid, the porbeagle shark *L. nasus*) were analyzed in the principal components analysis (PCA; **Tables 2 and 3**). We plotted the first two components (PC1, 54.6%; PC2, 26.8%), which provided >50% of the sum variance among these data (81.4%; **Fig. 8**), to 1) visually observe relationships among variables without confounding issues of ontogeny, body region, or stress axis, and 2) analyze variables across ecomorphotype groups. Component 1 was linked to toughness and strength along both stress axes while component 2 was related (but not significantly; 0.78) to stiffness. Of 12 variables, four significantly correlated (>0.8) along component 1 (PC1). Significant correlations indicate strong representation of that variable along the component [27,60]. PC1 was positively represented by increasing strength and toughness measurements (along both longitudinal and hoop stress axes; **Fig. 8**). Along PC2, skin stiffness stressed along the hoop axis approached a significant 0.8 threshold (0.78).

4. Discussion

We tested shark skin in uniaxial tension to failure and calculated the tensile strain and mechanical properties (strength, stiffness, and toughness) to evaluate the impact of ecological and ontogenetic factors on mechanical behavior. We used skin from 20 shark species to quantify the effects of ecomorphotype and ontogeny, as well as stress axis and body region. We used the bonnethead shark *Sphyrna tiburo* to quantify skin mechanics in a single species across an ontogenetic series. Finally, we analyzed principal component analysis to reduce the dimensionality among skin morphology and mechanical behavior to understand the

mechanisms that regulate skin function.

4.1 Does shark skin vary across ecomorphotypes?

We hypothesized that the mechanical behavior of shark skin would be specialized for the diverse habitats, migratory behaviors, and growth patterns of the different species, as these ecological factors may place specific mechanical demands on the skin. The denticle density, which is known to vary among species, we found ranged from 1–67 denticles per mm^2 and shark skin from Ecomorphotype A (benthic sharks) was less denticle-dense than skin from the other Ecomorphotypes (**Fig. 2A**), highlighting the ecological specificity of dermal denticles. These results are consistent with previous literature that denticles among benthic sharks, such as nurse sharks *Ginglymostoma cirratum*, are less densely arranged than faster, pelagic shark species [20,28,61]. The density and morphology of nurse shark denticles are well-suited for the benthic ecology and life history strategy of this species, including behaviors like resting on the ocean floor, burrowing into crevices for food, and swimming slower relative to other shark species [30]. The denticle crowns of nurse sharks are smooth and asymmetrical, and the denticles cover much of the integument surface, but are heavier and thicker than other benthic/sedentary shark denticles, suggesting they are protective [20,28,61]. Contrary to our hypothesis, sharks from Ecomorphotype A did not have the toughest skin, but they also did not differ statistically from Ecomorphotype E (night shark *Carcharhinus signatus*), which had skin ten times tougher than Ecomorphotypes B and C (**Fig. 6A**). Interestingly, the non-migratory nurse sharks of Ecomorphotype A had similarly extensible, stiff, and strong skin as the other ecomorphotypes. These results suggest that skin extension is more likely related to differences among body sizes (at maturity) than migratory behaviors. Additionally, tensile strain positively correlated with fork length (**Fig. 3D**) and was the only mechanical variable related to body size, supporting the positive relationship between body size and skin extensibility.

Skin thickness across sharks ranged from 0.4–4 mm, and species of carcharhinid sharks had the largest disparity, including the thinnest (Ecomorphotype B) and thickest (Ecomorphotype E) skin samples (**Fig. 2D**). These results are consistent with previous reports of variation in the stratum compactum layer thickness among species [1,6]. However, this much disparity within one clade of sharks may indicate

522 greater differences among the thicknesses and compositions of all skin layers (stratum compactum and
523 stratum laxum) than is currently understood [64]. Given the variability in denticle density and shark skin
524 thickness across ecomorphotypes, it seems that functional trade-offs predominantly modulate skin
525 morphology, and these differences do not seem to determine mechanical behavior. The small-bodied, non-
526 migratory sharks of Ecomorphotype B had 30% more denticles per mm than the large-bodied, migratory
527 species (Ecomorphotype D; **Fig. 2A**). The thinner skin and greater denticle densities of Ecomorphotype B
528 may indicate a functional benefit in small-bodied, non-migratory sharks, for which adjustable, overlapping
529 scales may be favorable for rapid turning and maneuverability. Small-bodied sharks of Ecomorphotype B
530 had skin that was 30% less extensible (~20%) than medium-bodied sharks (~30%, Ecomorphotype C) and
531 half as extensible as large-bodied, migratory sharks (~40%, Ecomorphotype D), indicating that skin
532 extensibility may be highly related to body size at maturity.

533 Conversely, pelagic species of carcharhinid and lamnid sharks (Ecomorphotypes C and D) are
534 faster and have denticles morphologically suited for drag reduction [15,19,20,23]. For example, silky sharks
535 *C. falciformis* are fast swimmers that have skin with high densities of adjustable, overlapping denticles with
536 thinner, lighter denticle crowns to accommodate for the increased density without reducing hydrodynamic
537 efficiency [15,20,62,63]. Medium-bodied sharks in Ecomorphotype C had an average skin stiffness that
538 was twice that of Ecomorphotype D, but neither group differed from the other ecomorphotypes (**Fig. 5A**).
539 Consistent with previous research, we found the range of collagen fiber angles in shark skin (45–65˚; **Fig.**
540 **S3**) was like the conserved range previously reported among species (40–60˚) [1,2,13]. This suggests that
541 stiffness (which results from collagen fiber arrangement) is relatively conserved apart from the medium-
542 bodied, migratory sharks (Ecomorphotype C), whose bodies may be specialized (more cylindrical in shape
543 and size) toward fiber angles that enhance skin stiffness and energy transmission down the body relative to
544 larger-bodied sharks. Species of large-bodied, migratory sharks (Ecomorphotype D) may also swim long
545 distances more efficiently with fewer, less overlapping scales as this could require less muscle contraction
546 and skin stiffening (**Table 1**). Additionally, larger-bodied sharks could benefit from thicker skin, which
547 may act as a "shock absorber" and prevent bursting due to large internal hydrostatic pressure changes from

548 muscle contractions [1,2]. Although thickness alone did not seem indicative of mechanical function, large
549 sharks of Ecomorphotype D may rely on energy stored in their thick skin to support their migratory
550 behavior, rather than high stiffness.
551
552 The deeper-water, non-migratory sharks (Ecomorphotype E; e.g., night shark *Carcharhinus*
553 *signatus*) had skin extension (60–80%) two to four times that of the small-bodied, non-migratory sharks
554 (Ecomorphotype B) and medium-bodied, migratory sharks (Ecomorphotype C; **Fig. 3A**). Ecomorphotype
555 E (night shark) had an average skin strength (~80 MPa) four times that of Ecomorphotypes B and D (~20
556 MPa; **Fig. 4A**). These results suggest that deep-water, medium-bodied species may require stronger skin
557 than the small-bodied and large-bodied shark species in Ecomorphotypes B and D, respectively. Strong
558 conclusions from the mechanical behavior of Ecomorphotype E are limited due to low sample size (N=1
559 shark). The high skin strength and toughness of this group could therefore be an effect of species, animal
560 maturity, or handling methodology. The night shark is a deep-water species that performs diel vertical
561 migration between 600–1200 meters depth and additionally exhibits dentition changes (heterodonty) among
562 ontogenetic stages [73,74,75,76]. Little is known about ontogenetic changes in the skin of the night shark,
563 so it is possible that this species could exhibit ontogenetic differences in skin mechanics as it does for
564 dentition. These changes could result in tougher skin from a mature night shark (measured here) relative to
565 a younger, immature night shark or compared with an individual of another species. Tougher skin could
566 benefit species that perform specific ecological behaviors, such as daily vertical migration to deeper depths,
567 by accommodating external pressure changes associated with continuously shifting depths that may
568 otherwise result in skin fractures. Some species have been recorded at depths >1000m, like deep diving
569 porbeagle and silky sharks, and these individuals had tough skin relative to the other study species
570 [77,78,79]. Comparisons with mechanical data of skin from deeper-water species, such as Greenland sharks
571 *Somniosus microcephalus,* would provide valuable context for answering these questions, albeit skin would
572 be difficult to obtain due to the habitat depth and long lives of these sharks.
573

574 Shark skin strength here ranged from 5–90 MPa, which coincides with the ranges reported for
575 coastal carcharhinid sharks (7–43 MPa) [33] and juvenile sharks (3–76 MPa) [13], as well as for spadenose
576 shark skin (24–32 MPa) [5] and similarly strong lesser devil ray *Mobula hypostoma* skin [65]. The strength
577 of shark skin here was consistent with other fish biological materials: elasmobranch vertebrae cartilage (4–
578 24 MPa), hagfish skin (21 MPa) and tendon (48 MPa), and osteichthyes skin (9 MPa) and tendon (30 MPa)
579 [50,66,67,68,69,70]. Notably, the higher end of the range of skin strength in this study is like the reported
580 strength of hagfish and bony fish tendon (more than these fishes' skin), highlighting the mechanical ability
581 of shark skin to function as a tendon. Skin stiffness here ranged between 1–550 MPa, a larger range than
582 previously reported for skin stiffness among juvenile (14.6–276.6 MPa) and coastal sharks (17–229 MPa)
583 [13; 33]. The larger range recorded here is consistent with the literature when considering the stiffness
584 values of Creager and Porter [33] do not include the high values of skin tested along the hoop axis (which
585 can double stiffness) and the immature age of sharks used by Creager and Porter and Hagood *et al.* [13].
586 Among juvenile sharks of three species, skin stiffness was conserved [13]. Despite the large range of
587 stiffness, there were few statistical differences among ecomorphotypes; Ecomorphotypes A, B, and E had
588 similarly stiff skin relative to one another and to Ecomorphotypes C and D. These data are consistent with
589 previous research [13,33] indicating shark skin is stiffer than osteichthyan skin (6–20 MPa) and tendon
590 (1.2–1.4 MPa) [12,66,67,70,71,72]. Notably, the ranges of stiffness do overlap across fishes. Relative to
591 bony fishes, the lower end of shark skin stiffness is equal to the Florida pompano *Trachinotus carolinus*
592 skin (4.4–19 MPa), which across three strain rates is stiffer than the skin of other teleost fish species [12].
593 Toughness here ranged two orders of magnitude from 0.5–50 MPa and is comparable to the higher end of
594 the range reported for silky shark skin (0.5–41 MPa) [13], and a wider range than published for coastal
595 sharks (2.5–16 MPa) [33]. As Ecomorphotype E had a sample size of one shark, let us consider the
596 toughness among the other ecomorphotypes. The other ecomorphotypes had similarly tough skin to each
597 other and as reported for coastal sharks [33]. Consistent with this trend in ecomorphological skin toughness,
598 Creager and Porter [33] reported no species or regional trends in toughness among the five species of coastal
599 sharks, and did also note that only 25% of tested samples yielded so the authors could not statistically

600 analyze toughness. Additionally, exact toughness measurements may differ from those of Creager and
601 Porter and Hagood *et al.* due to the immature age of specimens used in those studies [13,33] compared to
602 the mature individuals and diverse species incorporated in this study. This is particularly important to
603 consider as skin toughness does appear to differ significantly between immature and mature sharks
604 (discussed below).
605
606 *4.2 Does shark skin vary ontogenetically?*
607 Across all sharks, the skin of mature individuals was more extensible (**Fig. 3B**), stronger (**Fig. 4B**),
608 stiffer (**Fig. 5B**), and tougher (**Fig. 6B**) than skin from pups. Exploring these relationships in more detail,
609 we found that mature and immature bonnethead sharks had stronger and more extensible skin than pups,
610 although immature shark skin was not stiffer or tougher (**Fig. 7**). Based on these data, stiffness and
611 toughness remain consistent throughout ontogeny, whereas extensibility and strength seem to increase from
612 pups to immature sharks and then are sustained into maturity. Thus, the mechanical properties between
613 mature and immature sharks are similar, although toughness differed and the denticle density among
614 immature sharks was greatest. These results show that shark skin mechanics are comparable between
615 immature and mature sharks.
616 Across all sharks, denticle density varied among ontogenetic stages and was highest among skin
617 from immature sharks, followed by pups, and the least dense among mature sharks (**Fig. 2B**). This result is
618 consistent with ontogenetic differences in dermal denticle morphology and density reported for Portuguese
619 dogfish *Centroscymnus coelolepis* skin, whose denticle volume and surface area are negatively allometric
620 with body length [27]. Although the current study does not include species of squaliform sharks, denticle
621 development may follow similar ontogenetic trends among shark species of different orders. Among fast
622 swimming sharks with drag-reducing denticle morphology, denticle ridge spacing is consistent
623 ontogenetically, while the crown width (dorsoventral orientation) expands over time [19,28,61,63].
624 Additionally, although denticles are replaced, they do not grow at the same rate as a shark's body and are
625 not continuously replaced in the same way sharks' teeth are [19,23,80,81]. Therefore, denticles and

626 epidermal space seem to spread out, resulting in a lower denticle density among skin from mature sharks,
627 as we observed here across ecomorphotypes and among bonnethead sharks.
628 As sharks mature, they experience energetic costs associated with growth and repair, and
629 particularly related to reproduction, including copulatory biting [82,83,84,85,86,87,88,89]. Within the
630 ontogenetic case study of bonnethead shark skin, mature sharks had stronger, stiffer, tougher, and more
631 extensible skin than pups (**Fig. 7**). Individual body size (FL) correlated positively with skin extensibility,
632 but did not vary relative to strength, stiffness, or toughness. These results indicate that ontogenetic changes
633 can account for some of the increases in mechanical properties of shark skin. Stronger, stiffer, tougher skin
634 may provide better protection to mature sharks that experience environmental or reproductive injuries.
635 However, protection of a shark's body is more likely provided by the dermal denticles and greater skin
636 thickness of mature sharks (**Fig. 2E**), which may assist with efficient energy expenditure to transmit force
637 from contractions of increased muscle mass. These data suggest that ontogenetic and ecological factors may
638 have a greater role in moderating mechanical properties compared to impacts of body size or species.
639
640 *4.3 Is mechanical anisotropy conserved across sharks?*
641 Based on previously reported findings among shark and other fish skins that contain similar
642 collagen fiber arrangements, we predicted anisotropy of shark skin mechanical behavior
643 [1,2,5,11,13,24,50,65,71,90]. Consistent with previous research, shark skin behaved mechanically
644 anisotropic across and within each ecomorphotype (**Fig. 9**), and among bonnethead sharks (**Fig. 7**). Shark
645 skin was more extensible when stressed along the longitudinal axis (rostrocaudal, **Fig. 3C**), highlighting
646 that greater skin extension along the axis of undulation provides a mechanical benefit during swimming.
647 Shark skin was significantly stronger and stiffer when stressed along the hoop axis (dorsoventrally, **Figs. 4C**
648 **and 5C**), indicating greater resistance to deformation of skin along this axis to maintain internal hydrostatic
649 pressure and transmit energy down the body, especially during rapid or shifting swimming styles [1].
650 Among bonnethead sharks, skin was stiffer when stressed along the hoop axis but was not stronger. These
651 data indicate that mechanical differences in skin stressed along opposing axes are a direct result of the

collagen fiber organization, which create conserved anisotropy across shark species [1,2]. As in a pressurized cylinder, this organization maintains optimal hoop and longitudinal stresses along a shark's body to improve energy efficiency. Anisotropy was found within each ecomorphotype group. Skin from Ecomorphotype A showed the least variation of mechanical behavior between axes (i.e. it was the most isotropic along stress axes; **Fig. S3**), which may be related to the flatter and compressed body morphology of benthic sharks. Altogether, these anisotropic results support the hypothesis that shark skin is an exotendon because the skin is a connective, locomotory structure that 1) distributes stress through optimization of force along the longitudinal and hoop axes, 2) contributes to elastic recoil and energy recapture via lengthening and stiffening, and 3) functions as a mechanically advantageous whole-body external tendon structure [2,11].

In this study, toughness was the only mechanical property to exhibit isotropic behavior, as was previously reported for juvenile sharks among three carcharhinid species [13]. The skin of American eel *Anguilla rostrata* and several hagfish species behaves mechanically anisotropic in the opposing orientation relative to shark skin (stiffer along the longitudinal axis and more extensible circumferentially) but also exhibits isotropic toughness [50]. We posit that toughness is maintained between axes for a few reasons. First, toughness is the mathematical result of both high stress and strain, so shark skin is equally tough between the extensible (high strain) longitudinal axis, and the stiff and strong (high stress) hoop axis but may exhibit different results when multiaxial stress is applied as opposed to uniaxial stress examined here [91,92]. Toughness values here may be lower than would be measured in the skin of free-swimming sharks, as uniaxial testing accounts for one stress axis at a time and trade-offs between mechanical behaviors that impact toughness values along each axis would dampen toughness for both axes [92,93]. Additionally, fracture toughness (as measured here) is the stress required to propagate a crack through a material to failure; as a biological composite, shark skin has many layers of collagen which overlap and form a network to stop cracks from propagating to deeper layers [92]. Toughness may therefore be unrelated to the direction of applied stress, and more related to the number and material of stratum compactum vs stratum laxum layers within the skin (i.e., specific aspects of skin thickness), which could impact the distribution of stress

678 [1,5]. Although the thickness of each individual dermal layer was not recorded here, these measurements
679 would be particularly useful to consider in future research evaluating skin toughness. Among some bony
680 fishes (the skipjack tuna *Katsuwonus pelamis* and Norfolk spot *Leiostomus xanthurus*), the skin is not thick
681 enough to function as an exotendon despite being a crossed-fiber reinforced network [72].
682
683 *4.4 How does shark skin vary among body regions within the lateral mid-body?*
684 The morphology and mechanical properties of shark skin have been shown to vary among body
685 regions of individuals and among species, and these studies used skin from a wider variety of body locations
686 or analyzed anteroposterior body regions [5,33]. Based on trends in the literature, we predicted variability
687 among the morphology and mechanical behaviors of shark skin across regions of the body. Across skin
688 samples from dorsoventral regions within the lateral mid-body (between the two dorsal fins), we found
689 variation of denticle density, skin thickness, and mechanical toughness. Shark skin from the medial body
690 region was tougher than skin from the dorsal and ventral body regions (**Fig. 6C**). Additionally, skin from
691 the medial region was thicker and contained a lower denticle density than skin from the dorsal and ventral
692 body regions (**Fig. 2C and F**). These results suggest that within the lateral mid-body, tougher skin from the
693 medial region (which includes the lateral line) may be useful in transmitting force along the midline while
694 preventing bursting at the body's edge. The tougher, thicker skin in this region could also be evolutionarily
695 adaptive and provide protection to the vital lateral line system. Additionally, minimal variability in strength
696 and stiffness in the mid-body might accommodate for the lateral extension needed in this region of the body
697 during undulation, feeding and pregnancy [94]. Mechanical testing across a greater diversity of species
698 would help indicate whether differences in skin strength and stiffness are limited across body regions within
699 the lateral mid-body, or if similarities among these data are due to the uneven and mixed sample sizes used
700 here. For example, the skin stiffness of several bony fishes has been shown to vary among taxa and body
701 regions, increasing along the rostrocaudal body axis [12].
702
703 *4.5 What are the mechanisms that moderate shark skin mechanics?*

704 The relationships among variables in the PCA supported the trends observed among the entire
705 dataset (e.g., stress axis and ontogenetic effects are differentially responsible for governing certain
706 mechanical properties). These findings indicate that skin strength and toughness may be regulated by
707 different factors than material stiffness, which is moderated by the collagenous fiber matrix arrangement in
708 the skin (**Fig. 8**).

709 Previously, research on the relationships between the mechanical properties and denticle density of
710 shark skin has indicated potential connections between the density of denticles and skin stiffness and
711 toughness. Dermal denticles could increase the rigidity of the skin through interlocking and overlapping
712 [32], thereby impacting skin strength or toughness [13,33]. When shark skin was mechanically tested along
713 the longitudinal axis only, denticle density correlated positively with stiffness and negatively with
714 toughness [33]. When shark skin (from between the two dorsal fins) was tested in both longitudinal and
715 hoop stress axes, the denticle density positively correlated with skin strength and toughness [13]. Based on
716 these trends we hypothesized that dermal denticles, which are embedded in shark skin, would contribute to
717 skin strength and toughness when evaluated across both axes of stress. In bonnethead sharks, we found
718 mechanical behaviors did not relate to denticle density, indicating that within this species (which should
719 have similar denticle morphology) the decrease in density from immature to mature individuals does not
720 appear to limit or negatively impact mechanical behaviors of the skin. Low contributions of denticle density
721 and collagen fiber angles to shark skin mechanical function in the PCA suggest that skin morphology is not
722 as large of an effect in moderating mechanics as hypothesized (**Fig. 8**).
723

724 ## 5. Conclusion

725 The mechanical behavior of shark skin is driven by the arrangement of a conserved collagenous network,
726 and moderated by functional ecomorphotypes, ontogenetic stages, stress axes, body sizes and body regions.
727 Results from this study show that shark skin strength, toughness, and stiffness may be suited for specific
728 ecomorphological characteristics of the species. Across all 20 species and within the case study of
729 bonnethead sharks, mature sharks had stronger, stiffer, tougher, and more extensible skin than pups, which

indicates a potential developmental requirement for the skin to increase its capacity for mechanical work. Stress axis was a common significant effect and due to the arrangement of collagen fibers, the skin hyperextends parallel to the body axis (longitudinally) and becomes stronger and stiffer as energy is shifted perpendicular, or circumferentially, around and down the body. In this way, shark skin can function as an external tendon, assisting in mechanical work during swimming. These results represent data from a diverse sample of shark species, although they are limited by the uneven sample sizes and small number of species representing Ecomorphotypes A and E. A comprehensive analysis of mechanical properties from mature sharks, representative of a greater ecomorphological and phylogenetic diversity would provide more insight into the variation of skin mechanical behavior across sharks. Although such investigations may be difficult, studies examining the mechanical anisotropy of shark skin using species with bodies that deviate from a cylinder shape would be useful. These presented results offer validity in comparisons of shark skin mechanical behaviors between immature and mature individuals. Shark species have evolved combinations of skin morphology fine-tuned to specific ecologies and lifestyles, but the variation of skin mechanical properties appears to be closely tied to ecomorphotype and ontogenetic development across sharks, and not a direct result of morphological differences.

Acknowledgements

The authors thank collaborators at NOAA Fisheries (Apex Predators Program/NEFSC Narragansett Lab including Dr. Lisa Natanson), Mote Marine Lab (Sarasota, FL; Jack Morris), Florida FWCC, and Florida Keys Aquarium Encounters for specimens. We thank Dr. M. Laura Habegger and Dr. Stephen Kajiura for contributed specimens. We thank William (Doug) Werry for collecting mechanical data from two individuals. We thank members of the Florida Atlantic Biomechanics Laboratory for assistance with dissections and manuscript feedback, including Jamie Knaub, Aubrey Clark, Lauren Simonitis, Beth Bowers, Ivan Heerdegen, Delaney Frazier, Maria Uribe Mejia, Eden Sabag, Caroline Sullivan.

Funding

This work was supported in part by the National Science Foundation Career Award to M.E.P. (NSF IOS 194713), the Society for Integrative and Comparative Biology Grant in Aid of Research to M.E.H., and the National Save the Sea Turtle Foundation scholarships to M.E.H.

References

[1] P.J. Motta, Anatomy and Functional Morphology of Dermal Collagen Fibers in Sharks, Copeia, (1977) 454-464.
[2] S.A. Wainwright, F. Vosburgh, J.H. Hebrank, Shark Skin: Function in Locomotion, Science, 202 (1978) 747-749.
[3] S.A. Wainwright, Form and function in organisms, American Zoologist, 28 (1988) 671-680.
[4] W. Meyer, K. Neurand, R. Schwarz, T. Bartels, H. Althoff, Arrangement of elastic fibres in the integument of domesticated mammals, Scanning Microsc, 8 (1994) 375-90; discussion 391.
[5] M.D. Naresh, V. Arumugam, R. Sanjeevi, Mechanical behaviour of shark skin, 22 (1997) 431-437.
[6] W. Meyer, U. Seegers, Basics of skin structure and function in elasmobranchs: a review, Journal of Fish Biology, 80 (2012) 1940-1967.
[7] U. Seegers, W. Meyer, Grundlegendes zur Struktur und Funktion der Haut der Fische aus vergleichender Sicht, Kleintierpraxis, 15 (2009) 73-87.
[8] S.A. Wainwright, Mechanical design in organisms, Princeton University Press, 2020.
[9] J.H. Long Jr., K.S. Nipper, The importance of body stiffness in undulatory propulsion, American Zoologist, 36 (1996) 678-694.
[10] J.H. Long, B. Adcock, R.G. Root, Force transmission via axial tendons in undulating fish: a dynamic analysis, Comparative Biochemistry and Physiology Part A: Molecular & Integrative Physiology, 133 (2002) 911-929.
[11] J.H. Long Jr., M.E. Hale, M.J. McHenry, M.W. Westneat, Functions of fish skin: flexural stiffness and steady swimming of longnose gar Lepisosteus osseus, Journal of Experimental Biology, 199 (1996) 2139-2151.
[12] C.P. Kenaley, A. Sanin, J. Ackerman, J. Yoo, A. Alberts, Skin stiffness in ray-finned fishes: Contrasting material properties between species and body regions, Journal of Morphology, 279 (2018) 1419-1430.
[13] M.E. Hagood, J.R.S. Alexander, M.E. Porter, Relationships in Shark Skin: Mechanical and Morphological Properties Vary between Sexes and among Species, Integrative and Comparative Biology (2023).
[14] H. Pratt, Reproduction in the blue shark, Prionace glauca, Fishery bulletin, 77 (1979) 445-470.
[15] P. Motta, M.L. Habegger, A. Lang, R. Hueter, J. Davis, Scale morphology and flexibility in the shortfin mako Isurus oxyrinchus and the blacktip shark Carcharhinus limbatus, Journal of Morphology, 273 (2012) 1096-1110.
[16] M.V. Ankhelyi, D.K. Wainwright, G.V. Lauder, Diversity of dermal denticle structure in sharks: Skin surface roughness and three-dimensional morphology, Journal of Morphology, 279 (2018) 1132-1154.
[17] M.C. De Lima Viliod, B.D.S. Rangel, L.C. Rocha, J.F. Dos Santos Domingos, C.E. Malavasi-Bruno, A.F. De Amorim, I.S. Watanabe, A.P. Ciena, Ecomorphological, space, and mineral relations of dermal denticles in angular angel shark (Squatina guggenheim), Microscopy Research and Technique, 84 (2021) 2017-2023.
[18] N. Crooks, L. Babey, W.J. Haddon, A.C. Love, C.P. Waring, Sexual dimorphisms in the dermal denticles of the lesser-spotted catshark, Scyliorhinus canicula (Linnaeus, 1758), PLoS One, 8 (2013) e76887.
[19] W. Reif, Protective and hydrodynamic function of the dermal skeleton of elasmobranchs, 1978.
[20] W. Raschi, C. Tabit, Functional aspects of Placoid Scales: A review and update, 43 (1992) 123.

[21] G. Díez, M. Soto, J.M. Blanco, Biological characterization of the skin of shortfin mako shark Isurus oxyrinchus and preliminary study of the hydrodynamic behaviour through computational fluid dynamics, 87 (2015) 123-137.
[22] A.G. Domel, G. Domel, J.C. Weaver, M. Saadat, K. Bertoldi, G.V. Lauder, Hydrodynamic properties of biomimetic shark skin: effect of denticle size and swimming speed, Bioinspiration & Biomimetics, 13 (2018) 056014.
[23] M. Popp, C.F. White, D. Bernal, D.K. Wainwright, G.V. Lauder, The denticle surface of thresher shark tails: Three-dimensional structure and comparison to other pelagic species, Journal of Morphology, 281 (2020) 938-955.
[24] M.K. Gabler-Smith, D.K. Wainwright, G.A. Wong, G.V. Lauder, Dermal denticle diversity in sharks: novel patterns on the interbranchial skin, Integrative Organismal Biology, 3 (2021) obab034.
[25] G. Rincon, R. Mota, R. Mazzoleni, R. Lessa, M.F.D. Moura, P. Charvet, Dermal denticle variations on a newborn Roughskin Dogfish Centroscymnus owstonii (Chondrichthyes: Somniosidae) captured off northeastern Brazil with notes on ontogenetic differentiation, Regional Studies in Marine Science, 44 (2021) 101761.
[26] M. Fischer, G. Fraser, K. Cohen, Denticle morphology in the Pacific Spiny Dogfish, Squalus suckleyi, 2022.
[27] D.F. Vaz, T.M. Avery, M.K. Gabler-Smith, G.V. Lauder, The Denticle Multiverse: Morphological Diversity of Placoid Scales across Ontogeny in the Portuguese Dogfish, Centroscymnus coelolepis, and Its Systematic Implications, Diversity, 15 (2023) 1105.
[28] W.G. Raschi, J.A. Musick, Hydrodynamic Aspects of Shark Scales, Special report in applied marine science and ocean engineering, Virginia Institute of Marine Science: William & Mary, 1984.
[29] A. Lang, P. Motta, M.L. Habegger, R. Hueter, F. Afroz, Shark Skin Separation Control Mechanisms, 45 (2011) 208-215.
[30] L.J. Compagno, FAO species catalogue, Vol. 4, Sharks of the world, An annotated and illustrated catalogue of shark species known to date, Part 1. Hexanchiformes to Lamniformes, 1984.
[31] S.L. Hoffmann, S.M. Warren, M.E. Porter, Regional variation in undulatory kinematics of two hammerhead species: the bonnethead (Sphyrna tiburo) and the scalloped hammerhead (Sphyrna lewini), The Journal of Experimental Biology, 220 (2017) 3336-3343.
[32] M.A. Kolmann, D.R. Huber, M.N. Dean, R.D. Grubbs, Myological variability in a decoupled skeletal system: batoid cranial anatomy, Journal of Morphology, 275 (2014) 862-881.
[33] S.B. Creager, M.E. Porter, Stiff and tough: a comparative study on the tensile properties of shark skin, Zoology, 126 (2018) 154-163.
[34] B.J. Muus, P. Dahlstrøm, Meeresfische der Ostsee, der Nordsee, des Atlantiks: in Farben abgebildet und beschrieben: Biologie, Fang, wirtschaftliche Bedeutung, 1968.
[35] J.E. Randall, Size of the great white shark (Carcharodon), Science, 181 (1973) 169-170.
[36] F. Cervigón, W. Fisher, INPESCA, Catálogo de especies marinas de interés económico actual o potencial para América Latina, Parte, 1, 1979.
[37] A. Bass, L. Compagno, Odontaspididae, Smiths' Sea Fishes. Springer-Verlag, Berlin, 1986 104-105.
[38] F. Cervigón, R. Cipriani, W. Fischer, L. Garibaldi, M. Hendrickx, A. Lemus, R. Már-Quez, J. Poutiers, G.B. Robaina, B. Rodriguez; Fichas FAO de identificación de especies para los fines de la pesca, Guía de campo de las especies comerciales marinas y de aquas salobres de la costa septentrional de Sur América. FAO, Rome, Italy, 1992.
[39] L.J. Compagno, Systematics and body form, Johns Hopkins University Press, Baltimore, Maryland, 1999.
[40] L. Compagno, Sphyrnidae, Hammerhead and bonnethead sharks, FAO identification guide for fishery purposes, The Living Marine Resources of the Western Central Pacific, FAO, Rome, (1998) 1361-1366.
[41] L. Compagno, V. Niem, Order Carcharhinidae, Carpenter, KE & Niem, VH The Living Marine Resources of the Western Central Pacific, 2 (1998) 1312-1360.

[42] E. Murdy, R. Birdsong, J. Musick, D. Secor, Fishes of Chesapeake Bay, Reviews in Fish Biology and Fisheries, 8 (1998) 105-105.
[43] R. Bowman, C. Stillwell, W. Michaels, M. Grosslein, Food of northwest Atlantic fishes and two common species of squid (NOAA Technical Memorandum NMFS-NE-155), Woods Hole, Massachusetts, USA, 2000.
[44] L.J. Compagno, Sharks of the world: an annotated and illustrated catalogue of shark species known to date, Food & Agriculture Organization, 2001.
[45] M.S. Love, Resource inventory of marine and estuarine fishes of the West Coast and Alaska: A checklist of North Pacific and Arctic Ocean species from Baja California to the Alaska-Yukon border, US Department of the Interior, US Geological Survey, 2005.
[46] W. White, P. Last, J. Stevens, G. Yearsley, D. Fahmi, Economically important sharks and rays of Indonesia, [Hiu dan pari yang bernilai ekonomis penting di Indonesia], Canberra, Australia: Australian Centre for International Agricultural Research, 208 (2006).
[47] P.R. Last, Sharks and rays of Australia, 248 (2009).
[48] G.M. Cavanaugh, Formulae and Methods of the Marine Biological Chemical Room, Marine Biological Laboratory: Woods Hole, Massachusetts, 1975.
[49] M.S. Micozzi, Experimental Study of Postmortem Change Under Field Conditions: Effects of Freezing, Thawing, and Mechanical Injury, Journal of Forensic Sciences, 31 (1986) 953-961.
[50] E.B.L. Kennedy, R.P. Patel, C.P. Perez, B.L. Clubb, T.A. Uyeno, A.J. Clark, Comparative biomechanics of hagfish skins: diversity in material, morphology, and movement, Zoology, 145 (2021) 125888.
[51] S.A. Ranamukhaarachchi, S. Lehnert, S.L. Ranamukhaarachchi, L. Sprenger, T. Schneider, I. Mansoor, K. Rai, U.O. Häfeli, B. Stoeber, A micromechanical comparison of human and porcine skin before and after preservation by freezing for medical device development, Scientific Reports, 6 (2016) 32074.
[52] C. Crawford, Comparison of mechanical properties of skin from Pacific Hagfish, Eptatretus stoutii, and Penpoint gunnel, Apodichthys flavidus, University of Washington Student Papers, 2012.
[53] C.S. Shea-Vantine, K.A. Galloway, D.N. Ingle, M.E. Porter, S.M. Kajiura, Caudal spine morphology and puncture performance of two coastal stingrays, Integrative and Comparative Biology, 61 (2021) 749-758.
[54] K.A. Galloway, M.E. Porter, Mechanical properties of the venomous spines of Pterois volitans and morphology among lionfish species, The Journal of Experimental Biology, 222 (2019) jeb197905.
[55] C.A. Schneider, W.S. Rasband, K.W. Eliceiri, NIH Image to ImageJ: 25 years of image analysis, Nature methods, 9 (2012) 671-675.
[56] R. Pollom, J. Carlson, P. Charvet, C. Avalos, J. Bizzarro, M. Blanco-Parra, A.B. Bell-Lloch, M. Burgos-Vasquez, D. Cardenosa, A. Cevallos, Sphyrna tiburo, The IUCN Red List of Threatened Species, 3 (2020).
[57] A. Clark, M. Porter, T. Meredith, Morphometric analysis of the elasmobranch olfactory rosette, Journal of Morphology, 283 (2022) 1464-1477.
[58] J.T. Grady, L.M. Bower, C. Gienger, R.E. Blanton, Fish scale shape follows predictable patterns of variation based on water column position, body size, and phylogeny, Evolutionary Ecology, 36 (2022) 93-116.
[59] B. Husson, P.-M. Sarradin, D. Zeppilli, J. Sarrazin, Picturing thermal niches and biomass of hydrothermal vent species, Deep Sea Research Part II: Topical Studies in Oceanography, 137 (2017) 6-25.
[60] P.L. Williams, R.D. Beer, Nonnegative decomposition of multivariate information, arXiv (2010) preprint arXiv:1004.2515.
[61] W. Reif, Morphology and hydrodynamic effects of the scales of fast swimming sharks, Fortschr Zool, 30 (1985) 483-485.
[62] D. Bechert, W. Reif, On the drag reduction of the shark skin, 23rd Aerospace sciences meeting,

(1985) 546.
[63] W. Raschi, J. Elsom, Comments on the structure and development of the drag reduction-type placoid scale, Proceedings of the Second International Conference on Indo-Pacific fishes, Ichthyological Society of Japan, Tokyo, (1986) 392-407.
[64] O. Schuitema, P.J. Motta, J. Gelsleichter, M. Horton, M.L. Habegger, Histological comparison of shark dermis across various ecomorphologies, The Anatomical Record (2024).
[65] A. Rajaram, N. Ramanathan, The Tensile Properties of Ray Fish Skin, in: S. Saha (ed.) Biomedical Engineering I, Pergamon, 1982.
[66] E.L. Brainerd, Pufferfish inflation: functional morphology of postcranial structures in Diodon holocanthus (Tetraodontiformes), Journal of morphology, 220 (1994) 243-261.
[67] R.E. Shadwick, H.S. Rapoport, J.M. Fenger, Structure and function of tuna tail tendons, Comparative Biochemistry and Physiology Part A: Molecular & Integrative Physiology, 133 (2002) 1109-1125.
[68] A.P. Summers, T.J. Koob, The evolution of tendon—morphology and material properties, Comparative Biochemistry and Physiology Part A: Molecular & Integrative Physiology, 133 (2002) 1159-1170.
[69] M.E. Porter, J.L. Beltran, T.J. Koob, A.P. Summers, Material properties and biochemical composition of mineralized vertebral cartilage in seven elasmobranch species (Chondrichthyes), Journal of Experimental Biology, 209 (2006) 2920-2928.
[70] A.J. Clark, C.H. Crawford, B.D. King, A.M. Demas, T.A. Uyeno, Material properties of hagfish skin, with insights into knotting behaviors, The Biological Bulletin, 230 (2016) 243-256.
[71] M.R. Hebrank, Mechanical properties and locomotor functions of eel skin, The Biological Bulletin, 158 (1980) 58-68.
[72] M.R. Hebrank, J.H. Hebrank, The mechanics of fish skin: lack of an" external tendon" role in two teleosts, The Biological Bulletin, 171 (1986) 236-247.
[73] J.R. Thompson, S. Springer, Sharks, skates, rays, and chimaeras, US Department of the Interior, Fish and Wildlife Service, 1965.
[74] W. Raschi, J.A. Musick, L. Compagno, Hypoprion bigelowi, a synonym of Carcharhinus signatus (Pisces: Carcharhinidae), with a description of ontogenetic heterodonty in this species and notes on its natural history, Copeia (1982) 102-109.
[75] J.K. Carlson, E. Cortes, J.A. Neer, C.T. McCandless, L.R. Beerkircher, The status of the United States population of night shark, Carcharhinus signatus, 2008.
[76] A.N. Poscai, A.L.S. Casas, J.P.C. Da Silva, P. Lenktaitis, O.B. Gadig, Inside the mouth of sharks: Comparative data on the morphology of the oropharyngeal cavity, Zoologischer Anzeiger, 293 (2021) 282-291.
[77] D.J. Curnick, S. Andrzejaczek, D.M. Jacoby, D.M. Coffey, A.B. Carlisle, T.K. Chapple, F. Ferretti, R.J. Schallert, T. White, B.A. Block, Behavior and ecology of silky sharks around the Chagos Archipelago and evidence of Indian Ocean wide movement, Frontiers in Marine Science, 7 (2020) 596619.
[78] G. Skomal, H. Marshall, B. Galuardi, L. Natanson, C.D. Braun, D. Bernal, Horizontal and vertical movement patterns and habitat use of juvenile porbeagles (Lamna nasus) in the western north Atlantic, Frontiers in Marine Science, 8 (2021) 624158.
[79] O.F. Dixon, C. De Silva, B.T. Phillips, A.J. Gallagher, Expanded vertical niche for two species of pelagic sharks: depth range extension for the dusky shark Carcharhinus obscurus and novel twilight zone occurrence by the silky shark Carcharhinus falciformis, Environmental Biology of Fishes, 107 (2024) 231-236.
[80] K.J. Martin, L.J. Rasch, R.L. Cooper, B.D. Metscher, Z. Johanson, G.J. Fraser, Sox2+ progenitors in sharks link taste development with the evolution of regenerative teeth from denticles, Proceedings of the National Academy of Sciences, 113 (2016) 14769-14774.
[81] R.L. Cooper, E.F. Nicklin, L.J. Rasch, G.J. Fraser, Teeth outside the mouth: The evolution and development of shark denticles, Evolution & Development, 25 (2023) 54-72.

[82] T. Tricas, E. Le Feuvre, Mating in the reef white-tip shark Triaenodon obesus, Marine Biology, 84 (1985) 233-237.
[83] J.C. Carrier, H.L. Pratt Jr., L.K. Martin, Group reproductive behaviors in free-living nurse sharks, Ginglymostoma cirratum, Copeia (1994) 646-656.
[84] C. Harvey-Clark, W. Stobo, E. Helle, M. Mattson, Putative mating behavior in basking sharks off the Nova Scotia coast, Copeia (1999) 780-782.
[85] H.L. Pratt, J.C. Carrier, A review of elasmobranch reproductive behavior with a case study on the nurse shark, Ginglymostoma cirratum, Environmental Biology of Fishes, 60 (2001) 157-188.
[86] S.E. Smith, Leopard shark mating observed off La Jolla, California, Calif Fish Game, 91 (2005) 128-135.
[87] H.L. Pratt Jr., J.C. Carrier, Elasmobranch courtship and mating behavior, Reproductive biology and phylogeny of Chondrichthyes, CRC press, 2011.
[88] E.K. Ritter, R.W. Amin, Mating scars among sharks: evidence of coercive mating?, Acta ethologica, 22 (2019) 9-16.
[89] B.S. Talwar, M.E. Bond, S. Williams, E.J. Brooks, D.D. Chapman, L.A. Howey, R. Knotek, J. Gelsleichter, Reproductive timing and putative mating behavior of the oceanic whitetip shark Carcharhinus longimanus in the eastern Bahamas, Endangered Species Research, 50 (2023) 181-194.
[90] Kirti, S.S. Khora, Mechanical properties of pufferfish (Lagocephalus gloveri) skin and its collagen arrangement, Marine and Freshwater Behaviour and Physiology, 49 (2016) 327-336.
[91] S. Vogel, Cats' paws and catapults: Mechanical worlds of nature and people, WW Norton & Company, 2000.
[92] S. Vogel, Comparative Biomechanics (Princeton & Oxford), Princeton University Press, 2003.
[93] L. Vogel, W. Peukert, Breakage behaviour of different materials—construction of a mastercurve for the breakage probability, Powder Technology, 129 (2003) 101-110.
[94] E.W. Gudger, How difficult parturition in certain viviparous sharks and rays is overcome, Journal of the Elisha Mitchell Scientific Society, 67 (1951) 56-86.

985 **Table 1.** Descriptive information for shark specimens and sample sizes of each species with skin mechanically tested in
986 this study. Categorical traits including habitat, body size, and migratory nature were used to group species into functional
987 ecomorphotypes [30; 31]. Ecomorphotypes include A) benthic, non-migratory species; B) small-bodied, non-migratory
988 species; C) medium-bodied, migratory species; D) large-bodied, migratory species; E) deep-water medium-bodied,
989 non-migratory species.
990

Taxonomy	Scientific name	Common name	Taxonomic authority	N	FL (cm)	TL (cm)	Habitat	Mature TL (cm)	Migratory (M) or Not	Ecomorpho-type
Carcharhiniformes										
Carcharhinidae										
	Rhizoprionodon terraenovae	Atlantic sharpnose shark	(Richardson, 1836)	6	36–81	45–96	Demersal	85–90	N	B
	Carcharhinus acronotus	Blacknose shark	(Poey, 1860)	2	67–96.4	81.5–117	Reef-associated	103–137	N	B
	Carcharhinus limbatus	Blacktip shark	(Valenciennes, 1839)	3	96–148.6	114–179	Reef-associated	120–194	M	C
	Prionace glauca	Blue shark	(Linnaeus, 1758)	2	253–257	*	Oceanic-epipelagic	173–281	M	D
	Carcharhinus leucas	Bull shark	(Valenciennes, 1839)	4	39–54.5	48.5–66	Coastal-estuarine	180–230	M	D
	Carcharhinus obscurus	Dusky shark	(Lesueur, 1818)	1	220	*	Coastal-pelagic	220–300	M	D
	Carcharhinus isodon	Finetooth shark	(Valenciennes, 1839)	1	72.6	92.3	Demersal	119–139	M	C
	Negaprion brevirostris	Lemon shark	(Poey, 1868)	1	39	51	Reef-associated	239–340	M	D
	Carcharhinus signatus	Night shark	(Poey, 1868)	1	124.2	*	Benthopelagic	150–205	DVM	E
	Carcharhinus falciformis	Silky shark	(Bibron, 1839)	5	35–91.5	47–109	Oceanic-epipelagic	202–260	M	D
	Carcharhinus brevipinna	Spinner shark	(Valenciennes, 1839)	4	63–173	78–195	Reef-associated	170–266	M	D
	Galeocerdo cuvier	Tiger shark	Péron and Lesueur, 1822	1	297	359.6	Benthopelagic	210–350	M	D
Sphyrnidae										
	Sphyrna tiburo	Bonnethead shark	(Linnaeus, 1758)	8	20–63	24.5–80.7	Reef-associated	80–90	N	B
	Sphyrna mokarran	Great hammerhead shark	(Rüppell, 1837)	3	49–250.5	63.6–320	Coastal-pelagic	210–300	M	D
	Sphyrna lewini	Scalloped hammerhead shark	(Griffith and Smith, 1834)	1	42.6	58	Coastal-pelagic	140–273	M	C
Lamniformes										
Odontaspididae										
	Carcharias taurus	Sand tiger shark	Rafinesque, 1810	1	61	77.5	Reef-associated	220–230	M	D
Lamnidae										
	Carcharodon carcharias	White shark	(Linnaeus, 1758)	1	233	*	Oceanic	450–500	M	D
	Lamna nasus	Porbeagle shark	(Bonnaterre, 1788)	1	214.3	*	Oceanic	170–180	M	D
Alopiidae										
	Alopias vulpinus	Common thresher shark	(Bonnaterre, 1788)	1	57	117	Oceanic	226–400	M	D
Orectolobiformes										
Ginglymostomatidae										
	Ginglymostoma cirratum	Nurse shark	(Bonnaterre, 1788)	2	67.5–120	71–160	Reef-associated	230–240	N	A

991 *Denotes unknown value. FL (Fork length) and TL (Total length) are single values if N=1, and ranges when N>1. DVM = diel vertical migration
992
993
994
995
996

997 **Table 2.** Eigenvalues and percent variance for nine principal components (PCs, comp 1-9) in the PCA.

PC	eigenvalue	percentage of variance	cumulative percentage of variance
comp 1	6.55	54.60	54.62
comp 2	3.21	26.80	81.39
comp 3	1.27	10.60	91.99
comp 4	0.62	5.18	97.17
comp 5	0.21	1.76	98.92
comp 6	0.10	0.80	99.72
comp 7	0.02	0.19	99.92
comp 8	0.01	0.08	99.99
comp 9	0.00	0.00	100

998
999

Table 3 Descriptive information for all shark specimens used in this study (N=49), including individual fork length (FL) and total length (TL). Each shark denoted with an asterisk (*) contributed data for the PCA (N=10).

Shark Taxonomy	Common name	Sex	Maturity	FL (cm)	TL (cm)
CARCHARHINIFORMES					
Carcharhinidae					
Rhizoprionodon terranovae	Atlantic sharpnose	M	Immature	39.5	49
	Atlantic sharpnose*	M	Mature	81	96
	Atlantic sharpnose	M	Immature	44	54
	Atlantic sharpnose	M	Immature	36	45
	Atlantic sharpnose	M	Immature	44.5	55
	Atlantic sharpnose	F	Immature	45	56
Carcharhinus acronotus	Blacknose*	F	Mature	96.4	117.4
	Blacknose	F	Mature	67	81.5
Carcharhinus limbatus	Blacktip	F	Immature	96	114
	Blacktip*	M	Mature	148.6	179.3
	Blacktip	M	Mature	115	138
Prionace glauca	Blue	M	Mature	253.2	
	Blue*	M	Mature	257.1	
Carcharhinus leucas	Bull	M	Immature	54.5	65.5
	Bull	M	Pup	48	61
	Bull	F	Immature	53	66
	Bull	F	Pup	39	48.5
Carcharhinus obscurus	Dusky	F	Immature	220	
Carcharhinus isodon	Finetooth	M	Immature	72.6	92.3
Negaprion brevirostris	Lemon	M	Pup	39	51
Carcharhinus signatus	Night	F	Mature	124.2	
Carcharhinus falciformis	Silky	F	Immature	91.5	109.9
	Silky	M	Immature	84	101
	Silky	M	Immature	78.9	95.4
	Silky	F	Immature	83	99
	Silky	F	Pup	35	47
Carcharhinus brevipinna	Spinner	M	Immature	63	80
	Spinner	M	Immature	69.4	78
	Spinner	M	Immature	66	82
	Spinner*	F	Mature	173	195
Galeocerdo cuvier	Tiger*	F	Mature	297	359.6
Sphyrnidae					
Sphyrna tiburo	Bonnethead	M	Mature	53	62
	Bonnethead	F	Pup	20	24.5
	Bonnethead	F	Pup	20.5	26
	Bonnethead	M	Mature	50.2	63.3
	Bonnethead	M	Mature	47	60.5
	Bonnethead	F	Immature	48	58.4
	Bonnethead	F	Immature	51	64
	Bonnethead*	F	Mature	63	80.75
Sphyrna mokarran	Great hammerhead	M	Mature	204.5	265.7

	Great hammerhead	F	Immature	49	63.6
	Great hammerhead*	F	Mature	250.5	320
Sphyrna lewini	Scalloped hammerhead	F	Immature	42.6	58
LAMNIFORMES					
Odontaspididae					
Carcharodon taurus	Sand tiger	M	Pup	61	77.5
Lamnidae					
Carcharodon carcharias	White	M	Immature	233	
Lamna nasus	Porbeagle*	F	Mature	214.3	
Alopiidae					
Alopias vulpinus	Common thresher	M	Pup	57	117
ORECTOLOBIFORMES					
Ginglymostomatidae					
Ginglymostoma cirratum	Nurse	M	Immature	67.5	71
	Nurse	M	Immature	120	160

1003
1004

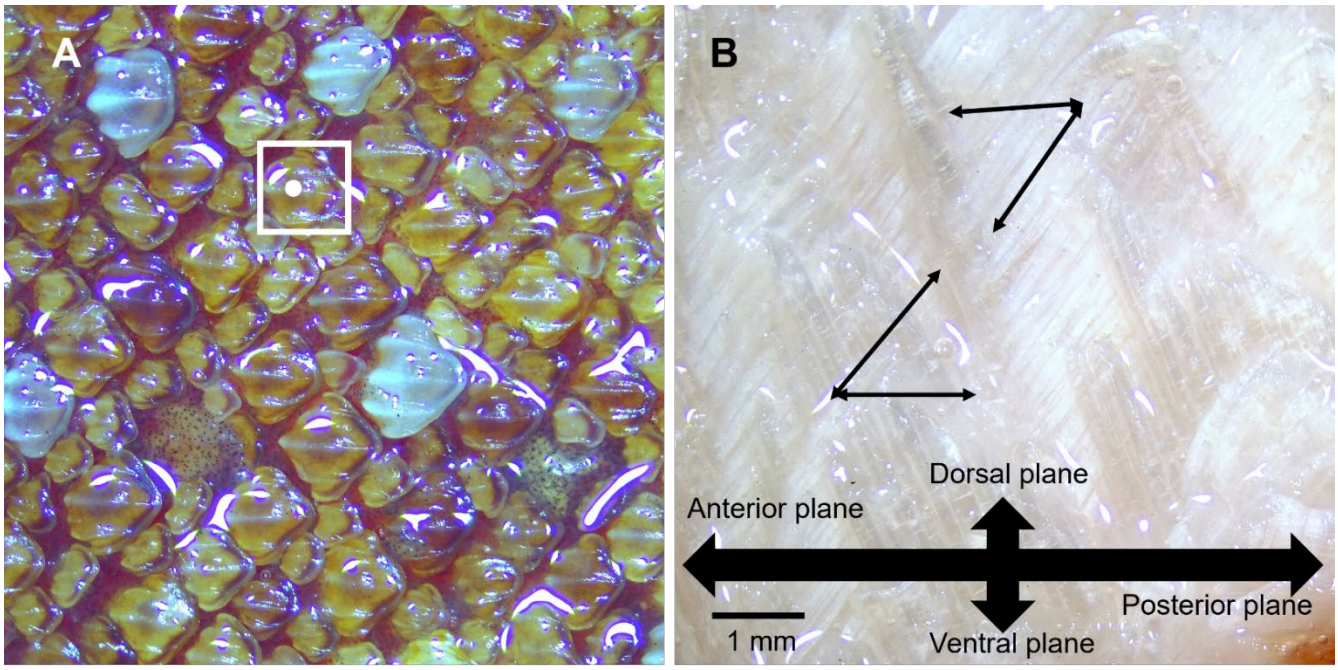

Fig. 1 Methodological analyses of skin morphology with images taken of nurse shark *Ginglymostoma cirratum* dorsal skin using stereoscopic microscopy (10x magnification). (A) Denticle density measurement example with 1x1 mm^2 white box for counting denticles, white dot marks the one denticle counted per mm^2. (B) Collagen fiber angle measurements (two angles extending from anteroposterior axis plane) in relation to directional planes. Fiber angles are shown as anteroventral and posterodorsal, although anterodorsal and posteroventral angles were also measured.

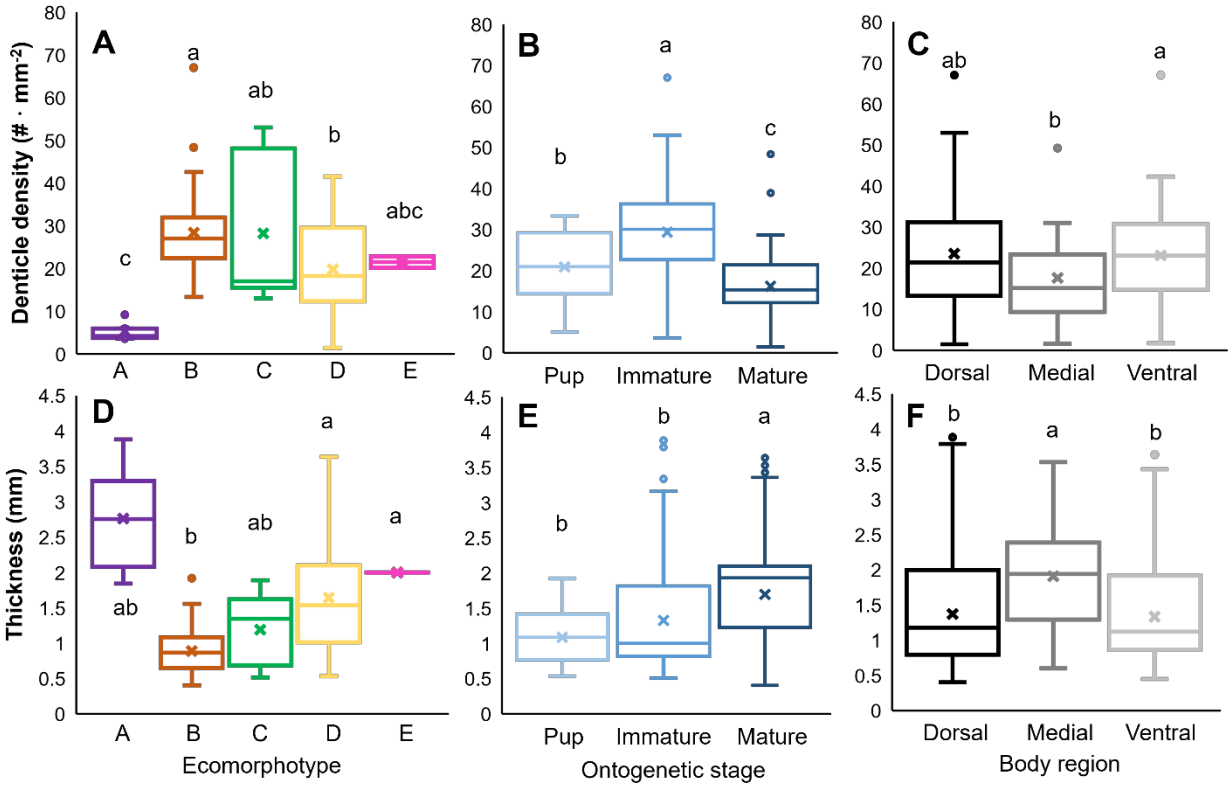

Fig. 2 Dermal denticle density and skin thickness vary among ecomorphotypes, ontogenetic stages, and body regions (A) Denticle density was greater among Ecomorphotypes B, C, and D than Ecomorphotype A (Kruskal-Wallis, $p<0.0001$). (B) Denticles were more densely arranged among immature sharks compared to pups and mature sharks (Kruskal-Wallis, $p<0.0001$). (C) Skin from the ventral and dorsal body regions had greater densities of denticles than skin from the medial body region (Kruskal-Wallis, $p=0.03$). (D) Ecomorphotypes D and E had thicker skin than Ecomorphotype B (Kruskal-Wallis, $p<0.0001$). (E) Mature sharks had thicker skin relative to the pups and immature sharks ($p<0.0001$). (F) Skin from the medial body region was thicker than skin from the dorsal and ventral regions (Kruskal-Wallis, $p=0.003$). Box edges are the first and third quartiles (25% and 75%, respectively), the line represents the median, the x is the mean, whiskers are values to the 97.5% quartile, and points outside the whiskers are values above the 97.5% quartile.

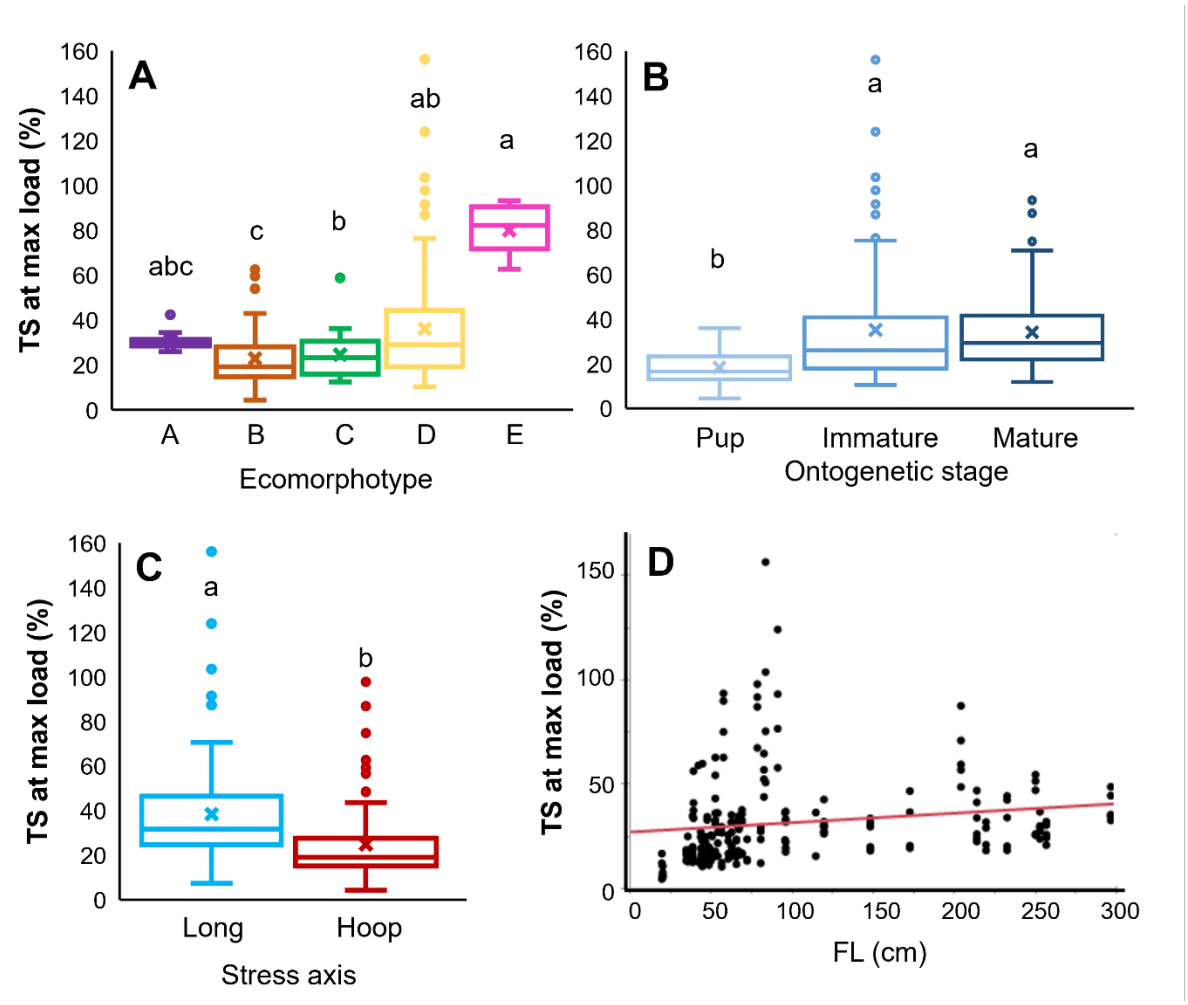

Fig. 3 Tensile strain at maximum load varies among ecomorphotypes and ontogenetic stages, between stress axes, and with fork length. (A) Extensibility varied among ecomorphotypes (Kruskal-Wallis, $p<0.0001$). (B) Mature and immature shark skin were more extensible than skin from pups (Kruskal-Wallis, $p<0.0001$). (C) Skin tested along the longitudinal axis (long, blue) was more extensible than along the hoop axis (red; Wilcoxon, $p<0.0001$). (D) Tensile strain correlated positively with body size (forklength, FL; $R^2=0.02$, $p=0.016$). Box edges are the first and third quartiles (25% and 75%, respectively), the line represents the median, the x is the mean, whiskers are values to the 97.5% quartile, and points outside the whiskers are values above the 97.5% quartile.

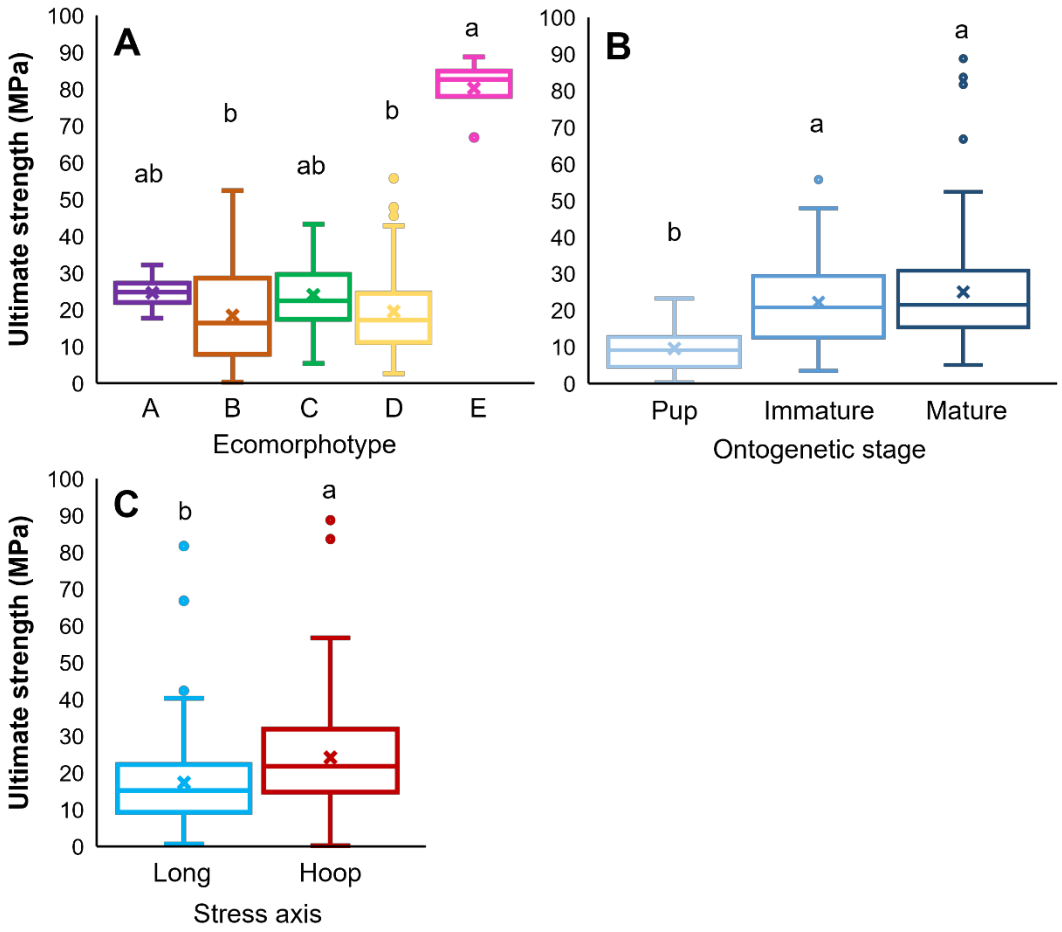

Fig. 4 Ultimate strength varies among ecomorphotypes and ontogenetic stages, and between stress axes. (A) Skin from Ecomorphotype E was stronger than Ecomorphotypes B and D (Kruskal-Wallis, $p=0.0003$). (B) Mature and immature sharks had stronger skin than pups (Kruskal-Wallis, $p<0.0001$). (C) Skin stressed along the hoop axis (red) was stronger than skin stressed longitudinally (long, blue; Wilcoxon, $p<0.0001$). Box edges are the first and third quartiles (25% and 75%, respectively), the line represents the median, the x is the mean, whiskers are values to the 97.5% quartile, and points outside the whiskers are values above the 97.5% quartile.

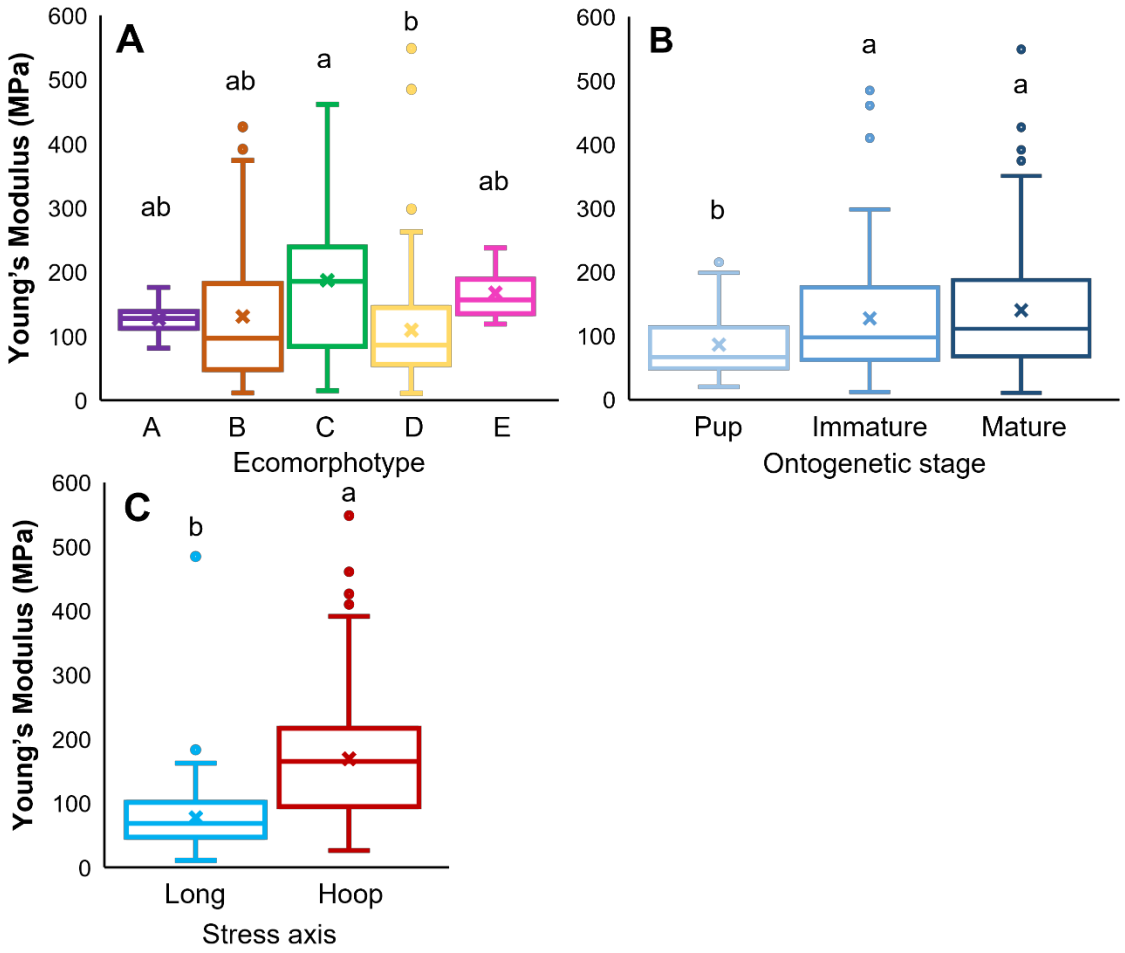

Fig. 5 Young's Modulus (stiffness) varies among ecomorphotypes and ontogenetic stages, and between stress axes. (A) Stiffness varied among ecomorphotypes, skin from Ecomorphotype C was stiffer than Ecomorphotype D (Kruskal-Wallis, $p=0.007$). (B) Mature and immature sharks had stiffer skin than pups (Kruskal-Wallis, $p=0.006$). (C) Skin stressed along the hoop axis (red) was stiffer than skin stressed along the longitudinal axis (long, blue; Wilcoxon, $p<0.0001$). Box edges are the first and third quartiles (25% and 75%, respectively), the line represents the median, the x is the mean, whiskers are values to the 97.5% quartile, and points outside the whiskers are values above the 97.5% quartile.

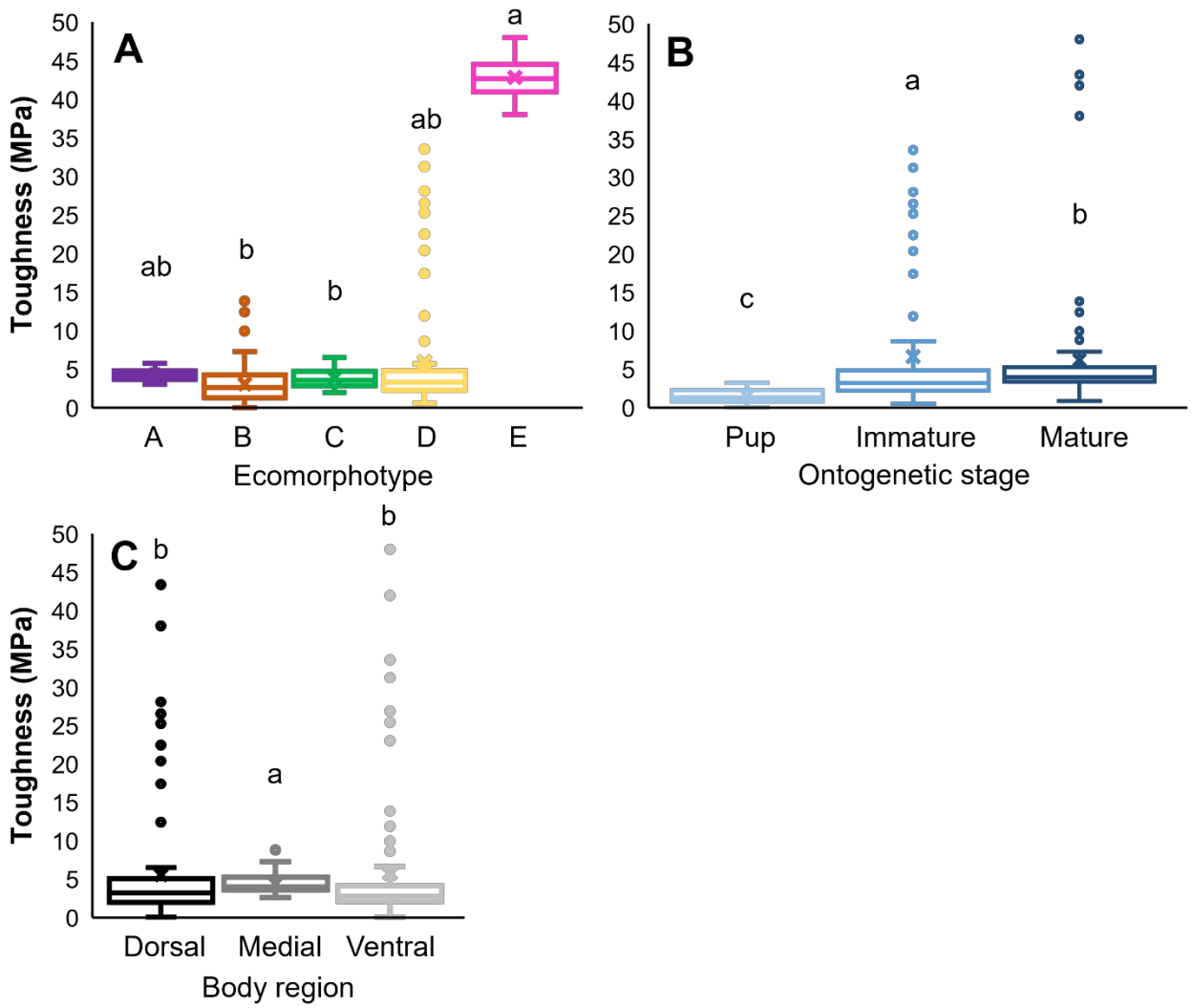

Fig. 6 Toughness varies among ecomorphotypes, ontogenetic stages, and body regions. (A) Shark skin from Ecomorphotype E was tougher than Ecomorphotypes B and C (Kruskal-Wallis, $p<0.0001$). (B) Mature and immature sharks had tougher skin than pups, and mature sharks had tougher skin than immature sharks (Kruskal-Wallis, $p<0.0001$). (C) Shark skin from the medial body region was tougher than the dorsal and ventral regions (Kruskal-Wallis, $p=0.004$). Box edges are the first and third quartiles (25% and 75%, respectively), the line represents the median, the x is the mean, whiskers are values to the 97.5% quartile, and points outside the whiskers are values above the 97.5% quartile.

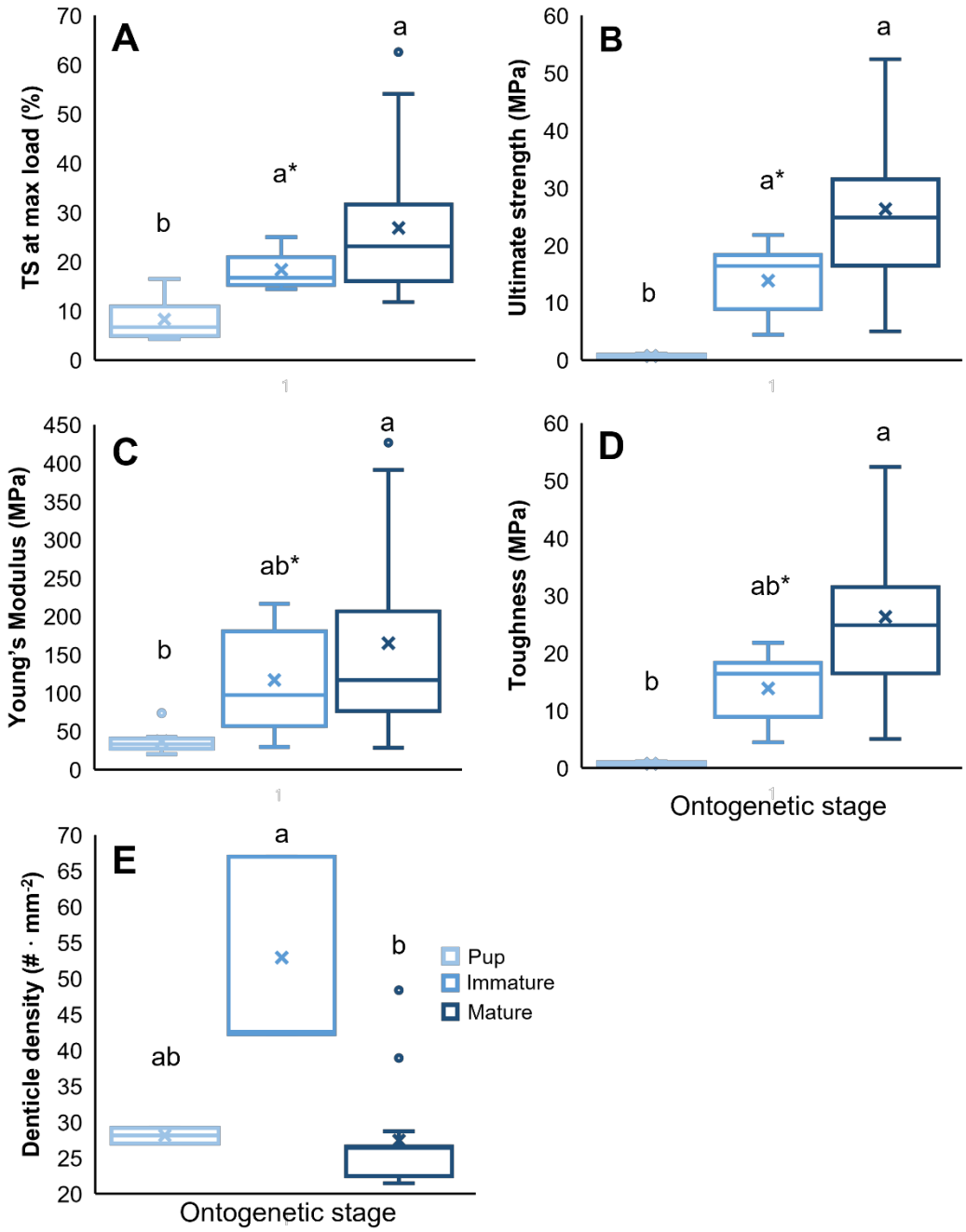

Fig. 7 Mechanical behaviors of the skin vary among ontogenetic stages in bonnethead sharks *Sphyrna tiburo*. Bonnethead shark skin (N=8 sharks, n=32 points) was mechanically greater among mature sharks (dark blue) compared to pups (light blue): (A) more extensible ($p=0.0004$), (B) stronger ($p<0.0001$), (C) stiffer ($p=0.001$), and (D) tougher ($p<0.0001$), relative to pup skin (Kruskal-Wallis tests). Immature shark skin mechanics were significantly (a*, $p=0.05$) or not significantly (ab*, $p=0.06$) greater than pup skin mechanical behavior. (E) Denticle density was higher among immature bonnethead sharks compared to mature sharks ($p=0.0001$), and intermediate among pups (Kruskal-Wallis, $p<0.0001$). Box edges are the first and third quartiles (25% and 75%, respectively), the line represents the median, the x is the mean, whiskers are values to the 97.5% quartile, and points outside the whiskers are values above the 97.5% quartile.

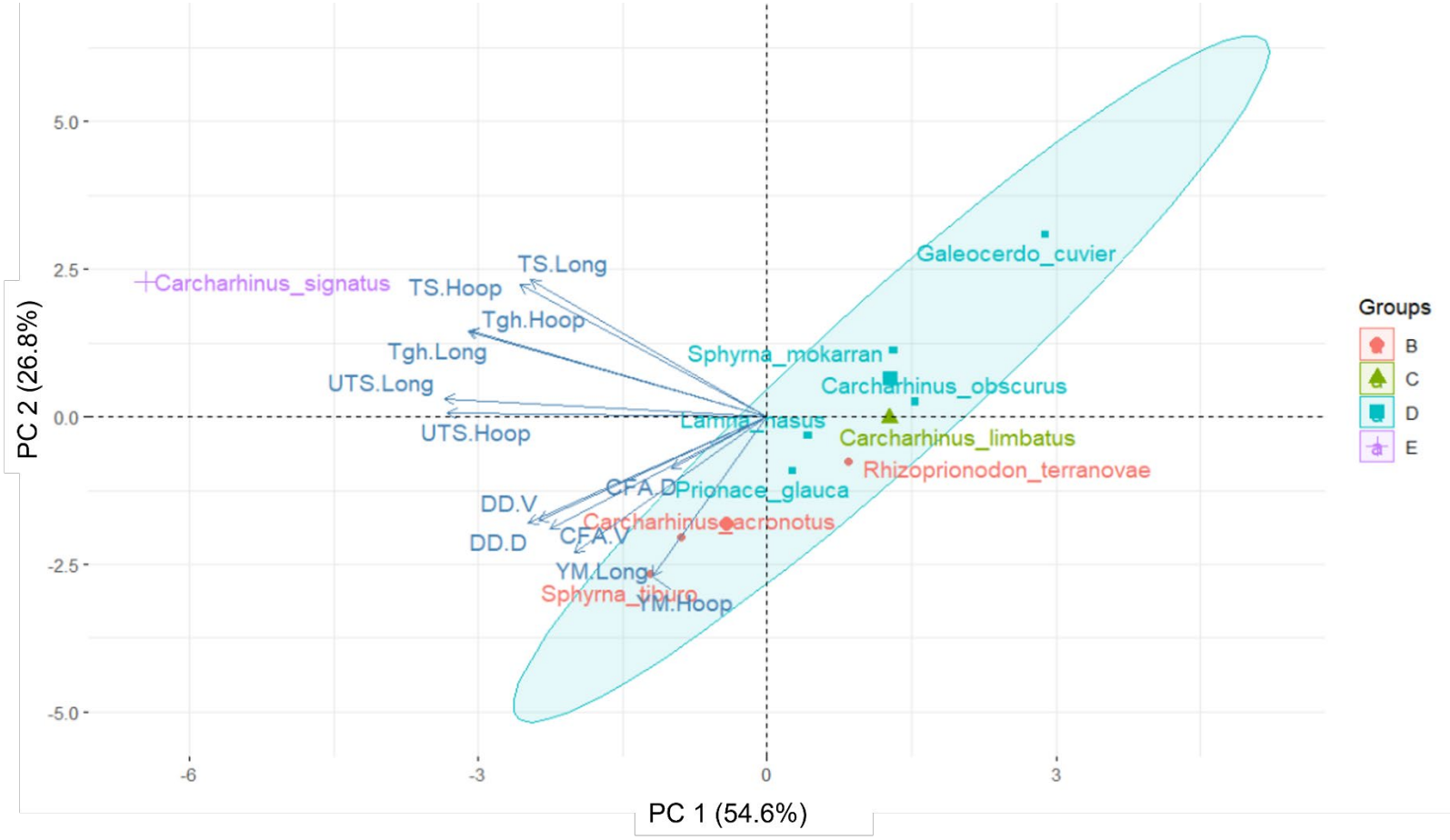

Fig. 8 Biplot of Principal Components Analysis (PCA) using data from 10 mature sharks (*n*=120). Individuals (species; colored points) across components 1 and 2 (**Tables 2 and 3**). Colors denote Ecomorphotypes: B, C, D, and E. Ecomorphotype A is not represented as there were no mature individuals within this ecomorphotype. Variables (blue arrows) examined were average denticle density and collagen fiber angle measures for dorsal (DD.D, CFA.D) and ventral (DD.V, CFA.V) body regions. Mechanical variables: extensibility (TS), strength (UTS), stiffness (YM), and toughness (Tgh) are averages along each stress axis (longitudinal, .Long and hoop, .Hoop).

Fig. 9 Anisotropic mechanical behavior within ecomorphotype groups. Shark skin from all five ecomorphotypes behaved mechanically anisotropic, indicating a conserved pattern of: (A) greater tensile strain (TS) at max load (extensibility, %) along the longitudinal (Long, blue) axis; (B) increased strength (MPa) along the hoop (Hoop, red) axis; and (C) increased stiffness (Young's Modulus, MPa) along the hoop axis. Box edges are the first and third quartiles (25% and 75%, respectively), the line represents the median, the x is the mean, whiskers are values to the 97.5% quartile, and points outside the whiskers are values above the 97.5% quartile.

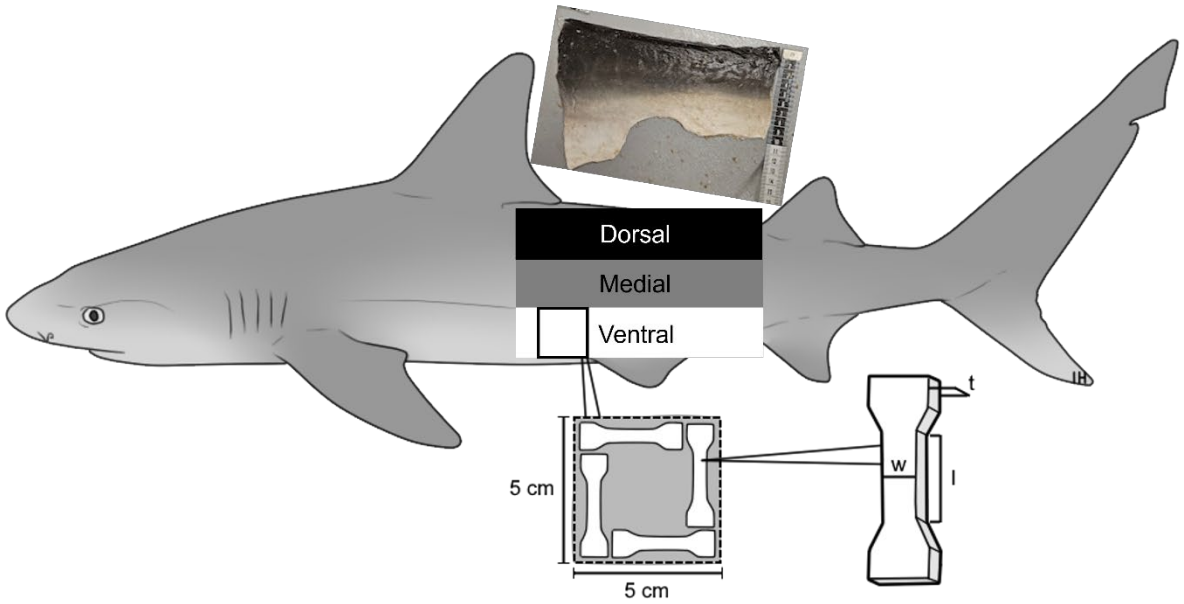

Fig S1 Diagram of shark skin dissection and removal of testing pieces. Skin was dissected from between the two dorsal fins and cut into squares (5x5 cm pop-out), each of which contained four testing pieces (two oriented along each axis of stress). Skin was categorized by body region as dorsal, medial, or ventral. Modified illustration by I. Heerdegen.

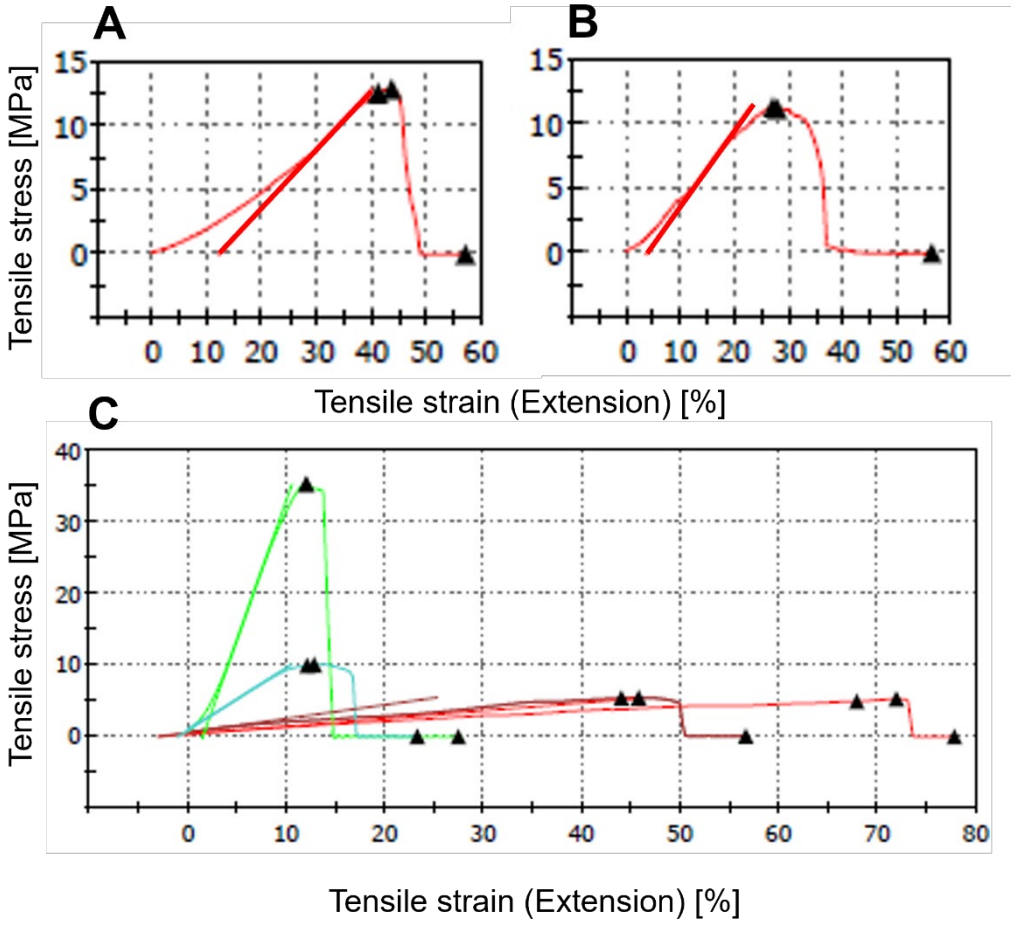

Fig. S2 Stress-strain curve examples. From the porbeagle shark *Lamna nasus*: individual A) longitudinal and B) hoop test curves. Red tangent lines have been defined for visibility. C) Scalloped hammerhead *Sphyrna lewini* curves from one skin square (4 tests; longitudinal = orange and red, hoop = green and blue. Black triangles denote (in order left to right): maximum load, yield point, and failure point. We did not use failure point for any metric in this study.

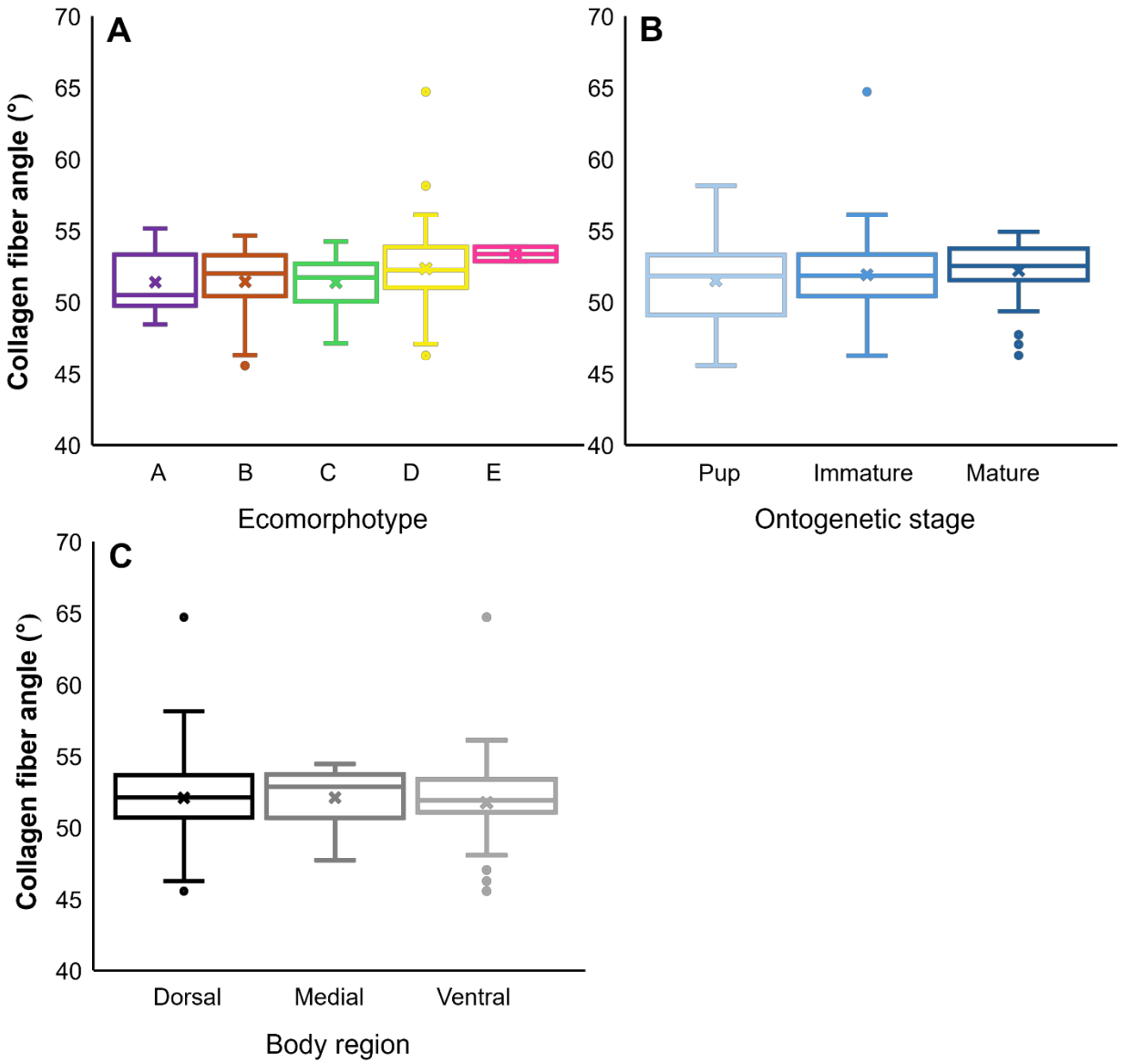

Fig. S3 Collagen fiber angles are conserved among ecomorphotypes, across ontogenetic stages and body regions. Collagen fiber angles did not significantly vary A) among ecomorphotype groups, B) across ontogenetic stages, or C) across body regions investigated. Box edges are the first and third quartiles (25% and 75%, respectively), the line represents the median, the x is the mean, whiskers are values to the 97.5% quartile, and points outside the whiskers are values above the 97.5% quartile.

List of Symbols and Abbreviations

A-P	anteroposterior; longitudinal axis ("Long")
D-V	dorsoventral; hoop axis ("Hoop")
CFA	collagen fiber angle (a measured angle from the body axis, reported in degrees)
DD	denticle density
TS	tensile strain (at maximum load, e.g. breaking extension)
UTS	ultimate tensile strength
YM	Young's Modulus; stiffness
Tgh	toughness (fracture)
SD	standard deviation
s.e.m.	standard error of the mean
SEM	scanning electron microscope
PCA	principal components analysis
MPa	megapascal(s)